Title

Top-down acetylcholine contributes to social discrimination via enabling action potentials in olfactory bulb vasopressin cells

Authors

Hajime Suyama, Veronica Egger, Michael Lukas

Institute of Zoology, Neurophysiology, University of Regensburg, 93040 Regensburg, Germany

Corresponding author

Michael Lukas

Institute of Zoology, Neurophysiology, University of Regensburg, 93040 Regensburg, Germany

e-mail: michael.lukas@ur.de

Abstract

Social discrimination in rats requires activation of the intrinsic bulbar vasopressin system, but it is unclear how this system comes into operation, as olfactory nerve stimulation primarily inhibits bulbar vasopressin cells (VPCs). Here we show that stimulation with a conspecific can activate bulbar VPCs, indicating that VPC activation depends on more than olfactory cues during social interaction. A series of *in-vitro* electrophysiology, pharmacology and immunohistochemistry experiments implies that acetylcholine probably originating from centrifugal projections can enable olfactory nerve-evoked action potentials in VPCs. Finally, cholinergic activation of the vasopressin system contributes to vasopressin-dependent social discrimination, since recognition of a known rat was blocked by bulbar infusion of the muscarinic acetylcholine receptor antagonist atropine and rescued by additional bulbar application of vasopressin. Thus, we demonstrated that top-down cholinergic modulation of bulbar VPC activity is involved in social discrimination in rats.

Introduction

Many mammals use olfactory cues as a fundamental communication tool, for the recognition and discrimination of individual conspecifics. A prominent example for a behavioral reaction that depends on olfaction-based discrimination of individuals is that ewes recognize the body odor of their own offspring and as a result, deny strange lambs to suckle [1]. Moreover, in prairie voles, the olfaction-based recognition of their mating partners enables them to establish monogamous pairbonds [2]. Rats and mice, the most common mammalian laboratory animals, also discriminate individual conspecifics via their odor signatures. This discrimination can then lead to various essential behavioral reactions [3]. To quantify the ability of rats to recognize individuals, so-called social discrimination tests are used [4]. Briefly, rats are exposed to a conspecific (sampling phase). After a short time of separation, rats are exposed to both, the same and a novel conspecific (discrimination phase). If the rats recognize the known conspecific, they investigate it less compared to the novel conspecific [4].

The peptidergic neuromodulator vasopressin (VP), an important mediator of various social behaviors in the mammalian brain [5], is a major player in facilitating social discrimination. For example, microinjection of VP into the OB enhances social discrimination [6]. Further, Tobin et al. [7] demonstrated the existence of an intrinsic bulbar VP system, consisting of VP-expressing cells (VPCs), and an impairment of social discrimination by the blockade of bulbar V1a receptors.

Recently, we classified these bulbar VPCs as non-bursting superficial tufted cells, featuring an apical dendritic tuft within a glomerulus, lateral dendrites along the top part of the EPL and extended axonal ramifications, mostly within the entire EPL[8]. The dense apical tuft implies that VPCs receive excitatory inputs from the olfactory nerve (ON) just like other bulbar cells with glomerular tufts such as mitral cells (MCs) [9], e.g. during sampling of a conspecific's body odors. Intriguingly, we found that electric ON stimulation elicits primarily inhibitory postsynaptic potentials (IPSPs) as recorded at the soma. This dominant GABAergic input masks a delayed barrage of excitatory postsynaptic potentials (EPSPs). Therefore, if ON activation inhibits

VPCs and thus cannot trigger VP release, it is unclear how intrinsic VP neurotransmission is at all possible during social discrimination. We hypothesize that to fully excite VPCs and allow VP release, non-ON inputs are required that either inhibit the GABAergic origin of the ON-evoked inhibition and/or deliver enough direct excitation to VPCs to outweigh the inhibition.

During social interaction, rats sample not only olfactory cues including urinary cues, but also other sensory cues, like vocalizations or touch [10]. Also, the sheer presence of a novel stimulus in their known environment may contribute to changes in their physiological and behavioral state. Thus, we suggest that states of arousal, attention, and/or the perception of non-olfactory cues during social interaction may be required for olfactory activation of bulbar VPCs. For the integration of such additional inputs into bulbar neurotransmission, top-down modulation is the most likely option. The most prominent modulatory centrifugal inputs to the OB are noradrenergic, serotonergic, and cholinergic fibers [11, 12, 13]. Those neuromodulatory systems were shown to be involved in changes of internal states [14, 15, 16], but more interestingly, they are also facilitators of social discrimination behavior, acting either directly in the OB or in other brain regions [17, 18, 19]. Thus, we propose them as candidate activators of the bulbar VP system. This notion leads to the following questions: (1) Are bulbar VPCs indeed activated during social interactions (although they are predominantly inhibited by activated olfactory afferents)? (2) Can any of the candidate centrifugal neuromodulators increase excitation of bulbar VPCs? (3) If so, is centrifugal modulation of bulbar VPCs involved in VP-dependent social discrimination? We approach these questions by investigating neuronal activity and synaptic mechanisms *in-vitro* as well as applying behavioral pharmacology *in-vivo*.

Results

Social interaction activates bulbar VPCs

As we recently demonstrated *in-vitro* [8] that ON stimulation alone primarily inhibits VPCs, we infer that bottom-up olfactory nerve input is unlikely to excite VPCs. On the other hand, during social discrimination VPCs should be strongly excited as VP neurotransmission was shown to be essential for this behavior [7]. To test this hypothesis, male juvenile VP-eGFP rats [20] were exposed to either, water (control) or one of two stimuli that are commonly used in social discrimination paradigms, i.e., rat urine or a novel juvenile rat [4]. We then compared the neuronal activity of bulbar VPCs between these different types of stimulation as reflected in phosphorylated extracellular signal-regulated kinase (pERK) induction in eGFP-labeled VPCs (Fig. 1a). The average section size of the main OB (MOB, water 4.48 ± 0.4 mm^2, urine 4.58 ± 0.3 mm^2, rat 4.85 ± 0.3 mm^2) and average number of $eGFP^+$ VPCs per section (water 81 ± 5 VPCs, urine 79 ± 5 VPCs, rat 85 ± 3 VPCs) were not different across animal groups (section size; p=0.723, ANOVA. $eGFP^+$ VPCs, Supplemental Fig. 1a; p=0.670, ANOVA, water n=10 rats, urine n=9, rat n=10)$_a$. While there is a substantial background of $pERK^+$ VPCs *in-vivo* (see discussion), indeed, the exposure to a rat resulted in significantly higher fractions of $pERK^+$ VPCs than the exposure to water. However, rat exposure did not differ significantly from urine exposure (Fig. 1c+d; p=0.038, ANOVA, rat vs. water p=0.011, rat vs. urine p=0.197, water vs. urine p=0.195)$_b$. These findings indicate (1) that bulbar VPCs are indeed excitable *in-vivo* and (2) that during social interaction additional yet unknown factors enable increased activation of VPCs.

The number of $pERK^+$ MCs was increased following the exposure to a rat compared to water or urine (Fig. 1b+e; p=0.042, ANOVA, rat vs. water p=0.025, rat vs. urine p=0.034, water vs. urine p=0.949)$_c$.

In addition, we analyzed activation of VPCs and mitral/tufted cells (M/TCs) in the accessory olfactory bulb (AOB), as the MOB and the AOB are both related to social discrimination in rats [21]. However, $pERK^+$ VPCs were rarely observed (Supplemental Fig. 1d; water 2.1 ± 0.7 % (0.4

124 ± 0.1 VPCs), urine 2.4 ± 0.8 % (0.5 ± 0.1 VPCs), rat 3.4 ± 0.8 % (1.0 ± 0.2 VPCs))$_d$ and the
125 fraction of pERK$^+$ VPCs was similar between the different groups (Supplemental Fig. 1d;
126 p=0.485, ANOVA, n=9 per group)$_e$. Thus, AOB VPCs are unlikely to play an important role in
127 facilitating social discrimination compared to MOB VPCs. The number of activated AOB M/TCs
128 was not different between groups (Supplemental Fig. 1f; p=0.164, ANOVA)$_f$.
129 Taken together, an increased activation of VPCs was found following social interaction, and
130 MOB VPCs showed more prominent activation than AOB VPCs. Thus, social interaction is
131 likely to involve additional inputs (beyond olfactory nerve input) that enable/unlock VPC
132 activation via modulation.

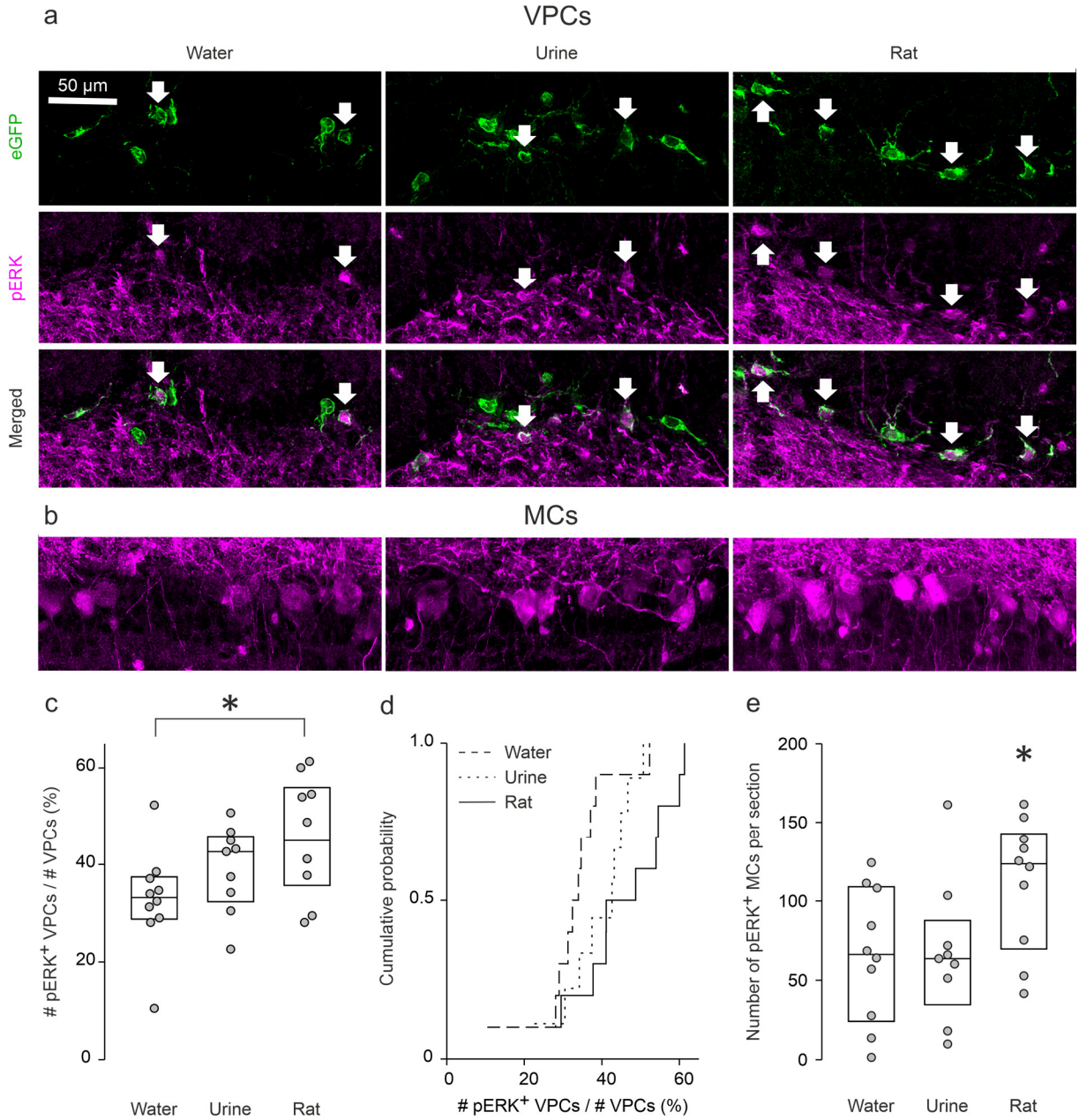

Fig. 1 **Social interaction activates bulbar VPCs**

(a+b) Representative average z-projections of the olfactory bulb that were immune-stained for eGFP (green, CF488) and pERK (magenta, CF 594). (a) VPCs. Arrows indicate cells that are double-labeled for eGFP and pERK. (b) pERK⁺ MCs. (c) Averaged fraction of number of pERK⁺ VPCs over number of number of VPCs in different stimulation groups (%). * $p<0.05$ rat vs. water. (d) Cumulative probability of averaged fraction of number of pERK⁺ VPCs over number of VPCs in different stimulation groups (%). (e) Averaged number of VPCs, of pERK⁺ VPCs or of pERK⁺ MCs per section in different stimulation groups. Data are presented as box-plots including median and distribution of single data points. ANOVA, LSD for single comparison, * $p<0.05$ vs. water and urine, n=10 (water), n=9 (urine), n=10 (rat). Scale bar, 50 µm.

143 **Cholinergic modulation triggers excitatory responses and action potentials during ON**
144 **stimulation of VPCs**
145
146 The OB, especially the glomerular layer (GL) and the external plexiform layer (EPL) where
147 VPCs are located, receives many centrifugal projections that release neuromodulators. These
148 projections originate from various brain areas [11, 12, 13]. The receptors of these neuromodulators
149 are expressed in the entire MOB [22, 23]. We hypothesized that such centrifugal neuromodulatory
150 inputs to the MOB could mediate the increased VPC activity that we observed during social
151 interaction. Thus we performed whole-cell patch-clamp recordings from VPCs and stimulated
152 the ON [8] while bath-applying neuromodulators (Fig. 2a).
153 Serotonin (5-HT,20 µM) decreased the amplitudes of ON-evoked IPSPs to 69.7 ± 10.1 % of
154 control (Fig. 2b+c; p=0.012, n=8 from 8 rats)$_g$. Noradrenaline (NA 20 µM) reduced IPSP
155 amplitudes to 62.9 ± 9.5 % of control (Fig. 2d+e; p=0.011, n=9 from 8 rats)$_h$. Thus, 5-HT and
156 NA modulation can reduce ON-evoked inhibition of VPCs but are unlikely to enable activation
157 of VPCs as observed during social interaction (Fig. 1).
158 In contrast, wash-in of ACh (100 µM) switched inhibitory to excitatory responses in the majority
159 of VPCs: 65 % of VPCs fired action potentials (APs, 13 out of 20 cells from 19 rats), 10 % of
160 VPCs responded with EPSPs to ON stimulation. The rest all showed decreased inhibition (Fig.
161 2f+g; p<0.001 for net response amplitude change towards positive/less negative values)$_i$.
162 Accordingly, the distribution of response amplitudes in the presence of ACh was significantly
163 different from control (Fig. 2h; p<0.001)$_j$, as well as different from the 5-HT or NA condition
164 (Fig. 2i; ACh vs. 5-HT p=0.003, ACh vs. NA p=0.002, 5-HT vs. NA p=1.0)$_k$. These excitatory
165 ACh effects were not due to an increased intrinsic excitability of VPCs since ACh did not alter
166 VPC AP spike frequencies during prolonged somatic current injections (Supplemental Fig.
167 2a+b; Treatment p=0.417, Current intensity p<0.001, Treatment*Current intensity p=0.528,
168 n=10 from 9 rats)$_l$. Moreover, an increased latency of the first spike was observed for lower
169 current injection levels, indicating rather reduced excitability during ACh treatment

170 (Supplemental Fig. 2a+c; Treatment p=0.080, Current intensity p<0.001, Treatment*Current
171 intensity p=0.015, ACh vs. ACSF (40 pA) p=0.029)$_m$.
172 Rat AOB M/TCs send axons to the dorsal MOB [24], and it was shown that pheromonal AOB
173 inputs are involved in social discrimination [21, 25]. To investigate whether AOB inputs can elicit
174 excitation in MOB VPCs, we electrically stimulated the AOB during whole-cell patch-clamp
175 recordings from MOB VPCs. Acute *in-vitro* slices for these experiments were prepared at a
176 cutting angle that should preserve the respective projections [24] (Supplemental Fig. 2d).
177 However, no VPC showed any responses (Supplemental Fig. 2e; n=21), suggesting that
178 modulation of MOB VPCs via AOB inputs is unlikely.
179 Taken together, we have identified ACh as a strong candidate neuromodulator that can unlock
180 VPC APs and thus enable axonal VP release in the MOB.

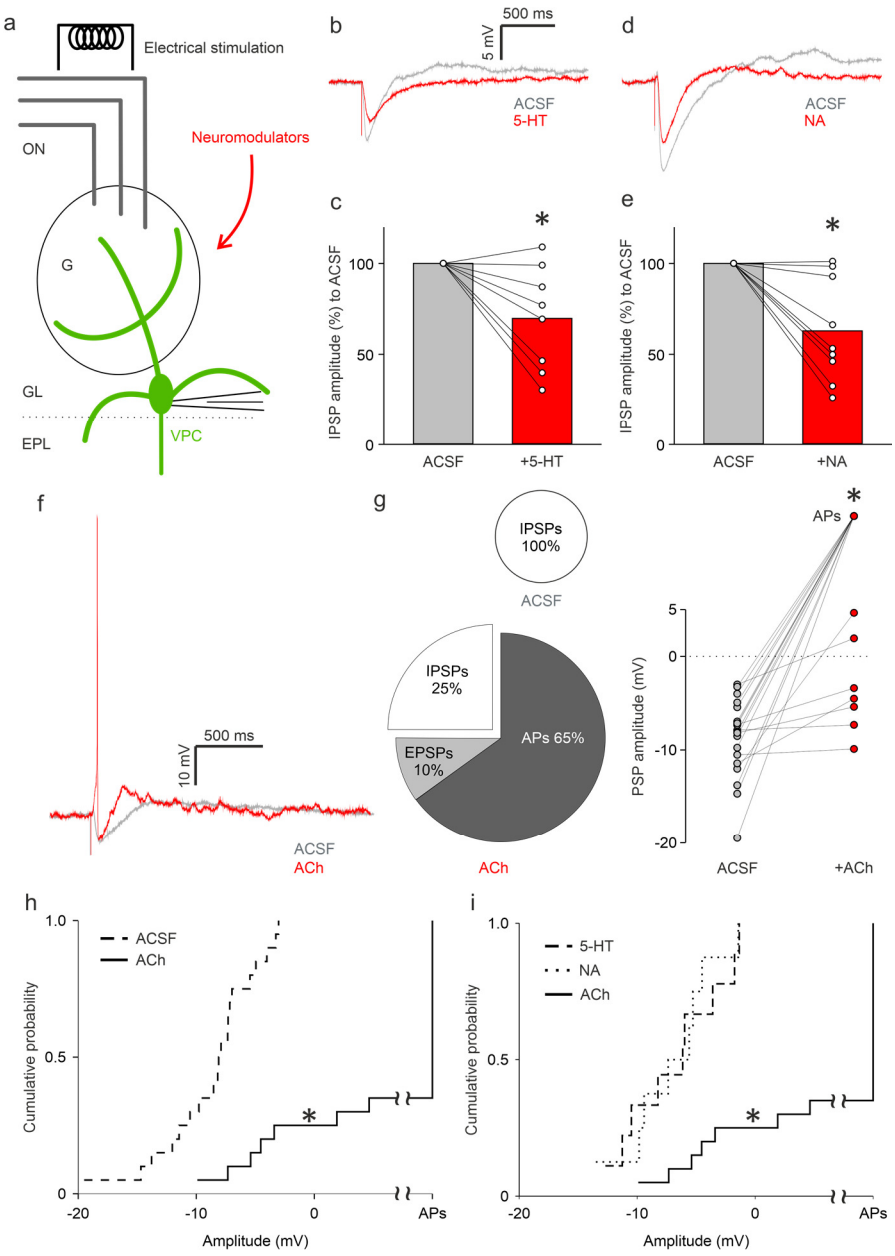

Fig. 2 **Cholinergic modulation triggers excitatory responses and action potentials during ON stimulation of VPCs**
(a) Schematic drawing of the experimental setup. Whole-cell patch-clamp recordings in 300 µm *in- vitro* slices of response from VPCs to electrical ON stimulation (50 µA, 100 µs, 30 s intervals) (b+d) Representative averaged traces of responses following ON stimulation in the ACSF condition (artificial cerebrospinal fluid, grey) and during bath application of 5-HT (20 µM) and NA (noradrenaline 20 µM, red). (c+e) Cumulative analysis of normalized IPSP amplitudes of evoked IPSPs to the ACSF control condition during bath application of 5-HT (n=8) and NA (n=9). Data are presented as means including distribution of single data points. Lines between data points represent related measurements. Related-Samples Wilcoxon Signed Rank Test, *p<0.05. (f) Representative averaged traces of responses to ON stimulation in the ACSF condition (grey) and a single trace during bath application of ACh showing APs (acetylcholine, red). (g) (left) Pie-charts represent the proportion of VPCs showing either APs, EPSPs or IPSPs in the ACSF and ACh condition. (right) Cumulative analysis of amplitudes of PSPs or APs (set as 100 mV) in the ACSF and ACh condition. Related-Samples Wilcoxon Signed Rank Test, *p<0.05. n=20. (h+i) Cumulative probability of evoked PSP amplitudes in the ACSF, 5-HT, NA or ACh condition (n=20/8/9/20). The amplitudes of APs were set as 100 mV. Kruskal-Wallis test for variation comparison, Bonferroni, *p<0.05 ACh vs. ACSF, 5-HT, NA.
ON, olfactory nerve. G, glomerulus. GL, glomerular layer. EPL, external plexiform layer. VPC, vasopressin cell.

197 **ACh modulates both ON-evoked inhibition and excitation but does not increase Ca^{2+}**
198 **influx into the apical dendrite**
199
200 For further dissection of the cellular underpinnings of these ACh effects, we quantified the
201 amplitude changes of evoked IPSPs in VPCs that did not turn into APs or EPSPs in ACh (5
202 out of 20 cells, Fig. 2g). In these 5 cells, ACh decreased the amplitudes of evoked IPSPs to
203 67.8 ± 11.3 % of control (Fig. 3a+b; p=0.043, n=5 from 5 rats)$_n$. This observation indicates that
204 ACh, like 5-HT and NA, also reduces inhibition of VPCs. We also examined the effect of ACh
205 on the isolated excitatory components of ON-driven inputs in VPCs. After the detection of
206 evoked IPSPs in ACSF, bicuculline, a GABA-A receptor antagonist, was applied to unmask
207 evoked EPSPs [8], followed by ACh administration. Half of VPCs occasionally showed evoked
208 APs under ACh application (Fig. 3d; 3 out of 6 cells from 5 rats). We averaged all subthreshold
209 traces and found that ACh application increased the amplitudes of evoked EPSPs to 204.4
210 ± 39.8 % from bicuculline alone (Fig. 3d; p=0.043, n=5 from 5 rats)$_o$. This increase in EPSP
211 amplitudes indicates that ACh enhances ON-evoked excitation to activate VPCs, on top of
212 reducing inhibition, possibly via acting on both excitatory and inhibitory glomerular neurons [26,
213 27]. In addition, we analyzed the onset of ON-evoked APs in VPCs triggered by ACh modulation
214 from Fig. 2 (8.6 ± 0.7 ms; n=12 from 12 rats, corresponding to Fig. 2g) and compared them to
215 the onset of evoked EPSPs in bicuculline alone, which was significantly slower (32.8 ± 12.1
216 ms; n=6 from 5 rats, corresponding to Fig. 3c; p=0.002)$_p$, further supporting the idea of
217 additional excitation by ACh.
218 Since VPCs innervate glomeruli via apical dendritic tufts [8] which are known to receive sensory
219 excitation in bulbar principal neurons, the mitral and tufted cells [9], ACh-mediated excitation
220 might act on processing within VPC tufts. To investigate subcellular processing in VPCs, we
221 simultaneously performed whole-cell patch-clamp recordings of PSPs from the soma and two-
222 photon Ca^{2+} imaging in the tufts and near the soma during ON stimulation (100 µM OGB-1,
223 Fig. 3e+f). In the control condition, a single ON stimulation was able to elicit Ca^{2+} influx in the
224 tufts but not in the proximal apical dendrite near the soma of VPCs (Fig. 3f+g; tuft vs. soma

225 p=0.002, n=8 from 8 rats)$_q$. However, upon ACh wash-in, although APs and EPSPs were
226 recorded at the soma, ACh did not further increase Ca^{2+} influx neither in the tufts nor the soma
227 (treatment p=0.203)$_q$. This observation implies that Ca^{2+} influx at the soma is not responsible
228 for the unlocking of somatic APs. Since 50 Hz-AP trains can elicit Ca^{2+} signals also close to
229 the soma in the proximal apical dendrites, the lack of such signals in response to single APs
230 in the presence of ACh is not a technical artefact but probably due to a very low density of
231 voltage-gated Ca^{2+} channels in these compartments, as known from hypothalamic VPCs [28]
232 (Supplemental Fig. 3b; ON/soma vs. 50Hz/soma p=0.014; n=8 from 8 rats)$_r$. Moreover, in the
233 imaging experiments (with 100 µM OGB-1 in the internal solution) there was no difference in
234 the effect of ACh on the increase of evoked PSPs compared to the previous
235 electrophysiological experiments (Supplemental Fig. 3c, p=0.456; n=9 vs. 11)$_s$ and therefore
236 this effect is independent of the potential buffering of postsynaptic Ca^{2+} by the Ca^{2+} indicator.
237 In conclusion, Ca^{2+} influx into the tuft or proximal apical dendrite appears to be neither required
238 for, nor modified by the ACh-mediated modulatory effects on ON-evoked postsynaptic PSPs.

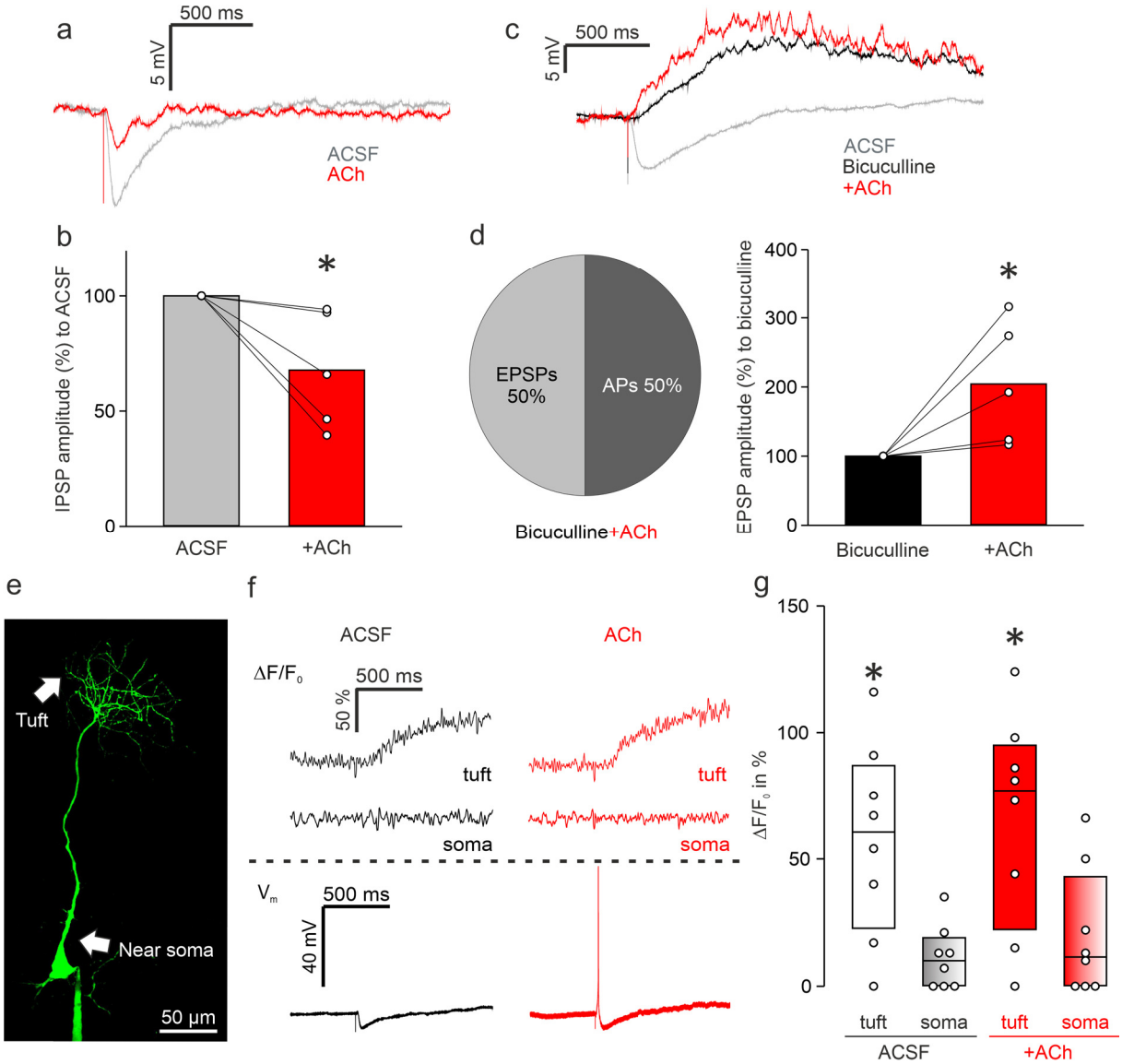

Fig. 3 **ACh modulates both ON-evoked inhibition and excitation via muscarinic receptors but does not increase intracellular Ca^{2+} influx**

Whole-cell patch-clamp recordings in 300 µm *in vitro* slices of response from VPCs to electrical ON stimulation (50 µA, 100 µs, 30 s intervals). (a) Representative averaged traces of responses following ON stimulation in the ACSF condition (grey) and during bath application of ACh (acetylcholine, red) showing reduced IPSPs. (b) Cumulative analysis of normalized evoked IPSP amplitudes to the ACSF condition during bath application of ACh (n=5). (c) Representative averaged traces of responses following ON stimulation in the ACSF condition (grey) and during bath application of bicuculline (50 µM, black) and additional application of ACh (100 µM, red). (d) (left) Pie-chart representing the proportion of cells showing either APs or EPSPs in the ACh condition (n=6). (right) Cumulative analysis of normalized evoked EPSP amplitudes to the bicuculline condition during additional application of ACh (n=5). (b+d) Related-Samples Wilcoxon Signed Rank Test, *p<0.05 vs. ACSF/bicuculline. (e) Representative picture of the VPC filled with OGB-1. Arrows indicate the tuft and the soma. Scale bar, 50 µm. (f) (top) Representative averaged traces of Ca^{2+} influx in the tuft and the soma. (bottom) Representative averaged traces of responses following ON stimulation (ACSF, black; ACh, red). (g) $\Delta F/F_0$ in % from baseline. Data are presented as box-plots including median and distribution of single data points. (2) × (2) mixed model ANOVA (location [within subject] × treatment [within-subject]), *p<0.05 vs. soma whithin the condition. n=8.

255 **Muscarinic signaling is the major player in reducing inhibition of bulbar VPCs**

256

257 To narrow down mechanisms of cholinergic excitation of VPCs, we next focused on ACh
258 receptor subtypes. The selective agonists (nicotine, 100 µM; muscarine, 1 µM) or antagonists
259 (mecamylamine, a nicotinic receptor antagonist, 20 µM; atropine, a muscarinic receptor
260 antagonist, 10 µM) were bath-applied to examine changes of ON-evoked PSPs in VPCs.
261 Unlike ACh application, nicotine application was not able to turn evoked IPSPs into excitation
262 in any of the tested VPCs (Fig. 4b; n=8 from 5 rats). Moreover, the average amplitude of
263 evoked IPSPs in nicotine was similar to control, even though variability across experiments
264 was high (Fig. 4a+b; p=0.327)$_t$. Similar results were observed with ACh application following
265 blockade of muscarinic signaling with atropine. Neither application of atropine alone nor the
266 atropine-ACh condition showed any evoked excitation and/or reduction of evoked-IPSP
267 amplitudes (Fig. 4c+d; p=0.156, Friedman test, n=7 from 4 rats)$_u$. Thus, nicotinic signaling is
268 most likely not sufficient to turn evoked inhibition to excitation in VPCs.
269 Conversely, muscarine administration enabled excitation in 25 % of VPCs (Fig. 4f; APs and
270 EPSPs in 1 cell each, n=8 from 5 rats). Furthermore, muscarine application significantly
271 reduced the amplitudes of ON-evoked IPSPs in the remaining 75% of cells (Fig 4f; p=0.028,
272 n=6 from 4 rats)$_v$. Intriguingly, application of mecamylamine followed by ACh, which isolates
273 muscarinic signaling, also resulted in ON-evoked excitation in a similar amount of VPCs as
274 during muscarine application (Fig. 4g+h; APs 18 % and EPSPs 9 % of cells, n=11 from 9 rats).
275 In addition, ACh following mecamylamine reduced evoked-IPSP amplitudes compared to
276 control or mecamylamine alone (Fig. 4h; p=0.034, Friedman test, mecamylamine-ACh vs.
277 ACSF p=0.024, mecamylamine-ACh vs. mecamylamine p=0.024, 73 % of cells, n=8 from 7
278 rats)$_w$ similar to muscarine application. Thus, these results indicate that the muscarinic
279 pathway is the major player in reducing inhibition of ON-stimulated VPCs, even though we
280 cannot entirely exclude the involvement of nicotinic signaling.

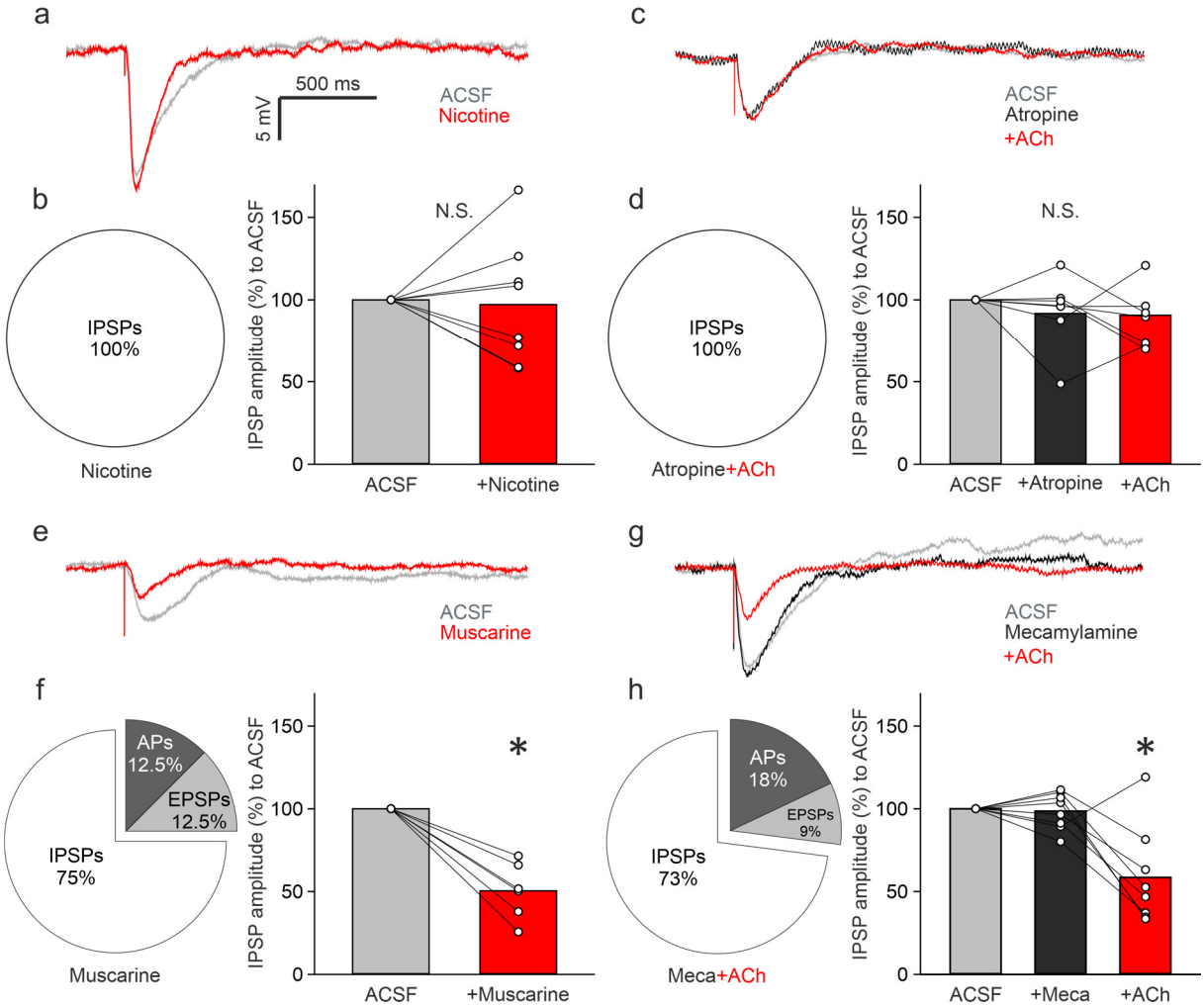

Fig. 4 **The muscarinic pathway is responsible for reduction of ON-evoked inhibition**

(a+e) Representative averaged traces of responses following ON stimulation in the ACSF condition (grey) and during bath application of nicotine/muscarine (100 µM/1 µM, red). (b+f) (left) Pie-chart representing the proportion of cells showing either APs, EPSPs or IPSPs in the nicotine/muscarine condition (n=8/8). (right) Cumulative analysis of normalized evoked IPSP amplitudes to the ASCF condition (n=8/6). Related-Samples Wilcoxon Signed Rank Test, *p<0.05 vs. ACSF. (c+g) Representative averaged traces of responses following ON stimulation in the ACSF condition (grey), during bath application of mecamylamine/atropine (20 µM/10 µM, black) and additional application of ACh (100 µM, red). (d+h) (left) Pie-chart representing the proportion of cells showing either APs, EPSPs or IPSPs in the antagonist-ACh condition (n=7/11). (right) Cumulative analysis of normalized evoked IPSP amplitudes to the ASCF condition during antagonist administration and additional bath application of ACh (n=7/8). Friedman test, Dunn for single comparisons, *p<0.05 vs. Meca (mecamylamine) or vs. ACSF. N.S., not significant.

293 **Cholinergic cells in the HDB are activated during social interaction**

294

295 Our results reveal that ACh can flip ON-evoked inhibition of bulbar VPCs into excitation *in-vitro*.
296 If this activating drive of ACh is indeed involved in triggering VPC excitation in behaving rats,
297 we hypothesized that ACh should be released into the OB during social interaction. Thus, ACh
298 neurons that are known to project to the OB from the horizontal limb of the diagonal band of
299 Broca (HDB) [29, 30] should get activated by social interaction. Activity of the cholinergic system
300 is correlated with changes in sensations or internal states such as arousal or attention [31, 32, 33,
301 34, 35, 36]. Moreover, it was shown that stimulation of HDB ACh projections into the MOB can
302 sharpen the odor responses of M/TCs [37, 38]. Since we had obtained whole brains from a subset
303 of the exposure experiments (water, rat urine, conspecific), we next investigated the activity of
304 ACh neurons in the HDB. To visualize activated HDB neurons and specifically activated ACh
305 neurons, we stained the HDB against pERK and choline acetyltransferase (ChAT) (Fig. 5a).
306 The total number of $pERK^+$ HDB cells was not significantly different between all groups (Fig.
307 5b; p=0.104, ANOVA, water n=5, urine n=5, rat n=6)$_x$. However, the number of $pERK^+$ ACh
308 neurons in the rat exposure group was significantly higher than that in the urine exposure group,
309 even though the $pERK^+$ ACh neuron number in the rat exposure group was not higher than
310 that in the water exposure group (Fig. 5c; p=0.034, ANOVA, rat vs. urine p=0.011, rat vs. water
311 p=0.113, water vs. urine p=0.255)$_y$. The results indicate that HDB ACh neurons are activated
312 more easily by social interactions than by investigating urine and thus more likely to excite
313 VPCs specifically during social interactions.

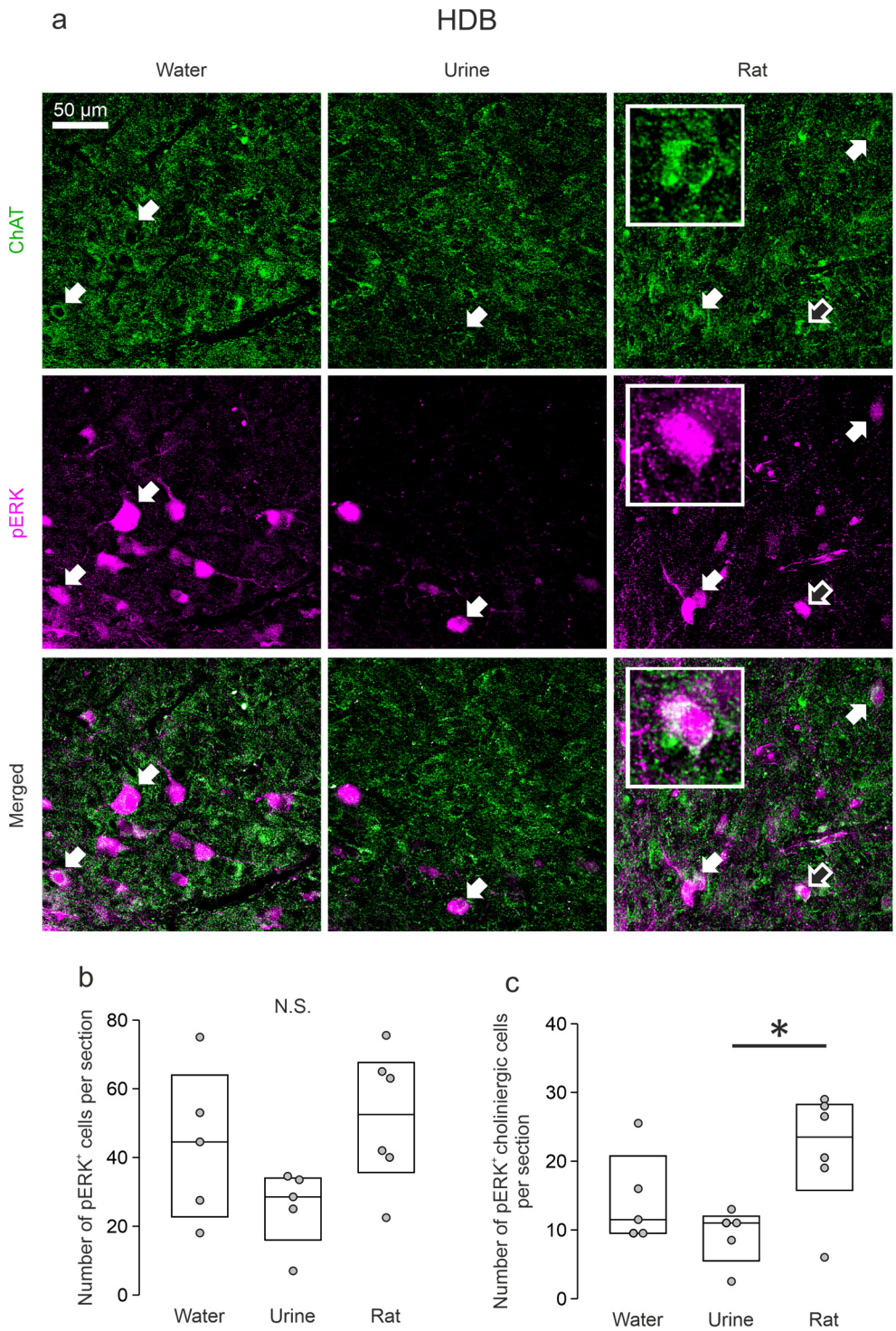

Fig. 5 **Cholinergic cells in the HDB are activated during social interaction**

(a) Representative average z-projections of the HDB (horizontal limb of the diagonal band of Broca) that were immune-stained for ChAT (choline-acetyltransferase, green, CF488) and pERK (magenta, CF 594). Arrows indicate cells that are double-labeled for pERK and ChAT. Insets show enlarged pictures of the cell indicated by blank arrows. Scale bar, 50 µm. (b+c) Averaged number of pERK$^+$ cells or pERK$^+$ cholinergic cells per section in different experimental groups. Data are presented as box-plots including median and distribution of single data points. ANOVA, LSD for single comparisons, *$p<0.05$ Rat vs. Urine, n=5 (water), n=5 (urine), n=6 (rat).

323 **Atropine-induced impairment of social discrimination is rescued by VP microinjection**
324 **into the OB in male rats**
325
326 Our data so far demonstrated a disinhibitory effect of bulbar ACh on ON-evoked VPC activity
327 mainly via muscarinic receptors as well as the activation of both systems, intrinsic bulbar VP
328 and HDB ACh, during social interaction. These observations are in line with behavioral studies
329 that demonstrate that pharmacological blockade of bulbar V1a receptor or systemic ACh
330 activity diminishes social discrimination abilities in rats [7, 39]. To examine if the cellular
331 mechanisms we observed in the OB indeed play a role for social discrimination in behaving
332 rats, we tested (1) if the blockade of muscarinic ACh signaling in the OB impairs social
333 discrimination and (2) if a later additional VP injection, mimicking potential ACh-facilitated VP
334 release, can rescue a possibly impaired behavior. Thus, we performed microinjections of
335 atropine (1 µg/ 1 µL per hemisphere) or vehicle (ACSF, 1 µL per hemisphere) followed by
336 either VP (1 ng/ 1 µL per hemisphere) or vehicle before the sampling phase of a social
337 discrimination test (Fig. 6a). In this test, the ability to discriminate two individuals is measured
338 in terms of how long rats investigate a novel versus a known stimulus rat [4].
339 Control rats that received only vehicle investigated the novel stimulus rat significantly more
340 than the known rat, indicating intact social discrimination (Fig. 6d; $p=0.033$, $n=13)_z$. In contrast,
341 atropine-injected rats showed a similar duration of investigation towards both, novel and known
342 stimulus rats (Fig. 6e; $p=0.240$, $n=14)_{a1}$. Thus, the blockade of muscarinic signaling in the OB
343 indeed impaired social discrimination. Atropine-VP injected rats, however, significantly
344 preferred investigating the novel stimulus rat over the known one (Fig. 6f; $p=0.031$, $n=14)_{b1}$.
345 Hence, impairment of social discrimination by atropine is most likely caused by a disruption of
346 the activation of the bulbar VP system, and in turn a reduced bulbar VP release during social
347 interaction. Therefore, their ability to discriminate a known from a novel stimulus was rescued
348 by additional VP injection.

This final experiment thereby supports our hypothesis based on our findings *in-vitro* that the activity of the bulbar VP system (that is essential for social discrimination) is triggered by centrifugal ACh inputs during social interaction.

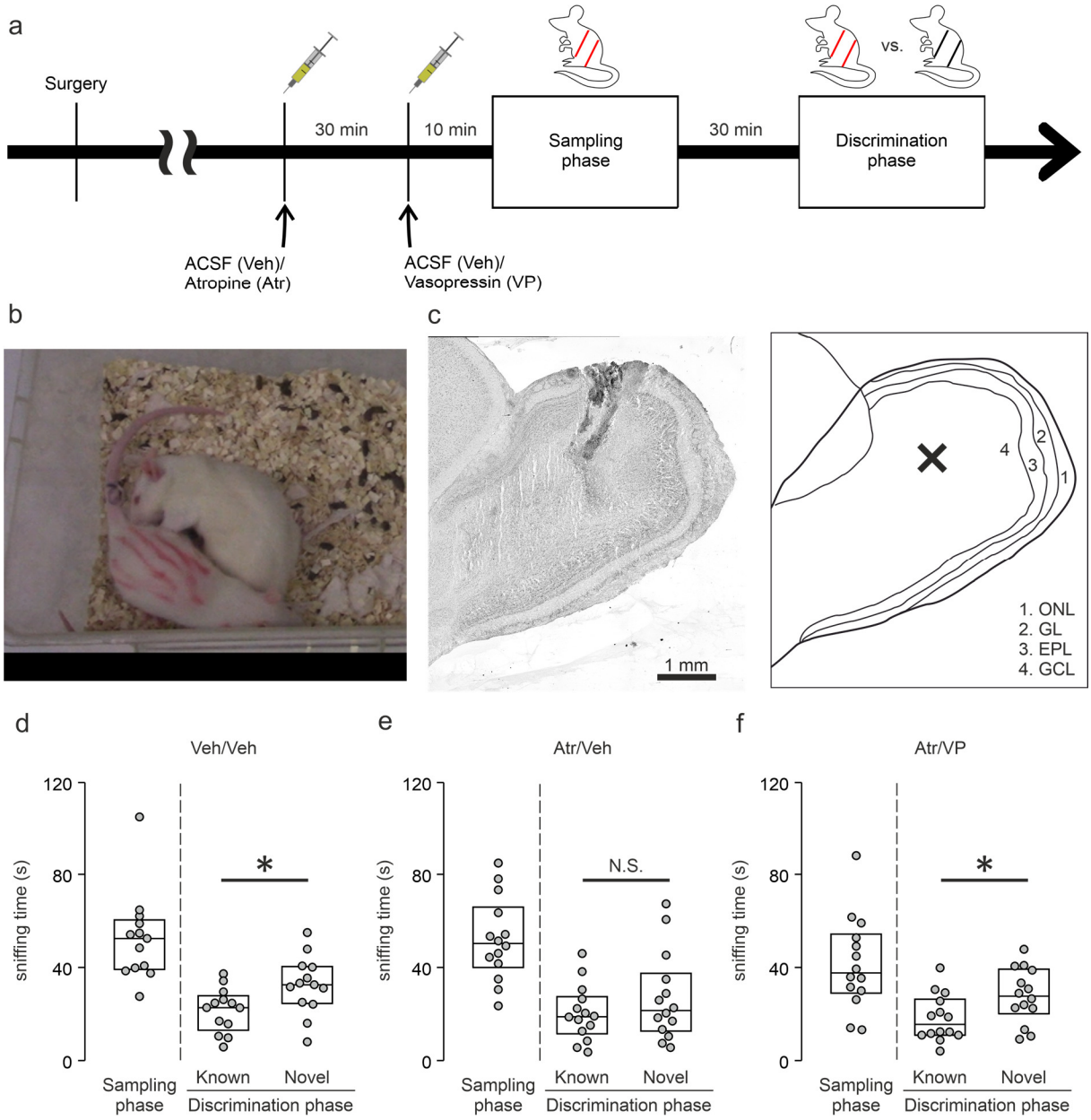

Fig. 6 **VP microinjection into the OB rescues the atropine-induced impairment of social discrimination in male rats** (a) Schematic time course of the experimental design. (b) Rat (5 weeks) without markings representing anogenital sniffing toward a stimulus rat (3 weeks) with red markings. (c) (left) Representative picture of the OB with dye injection via injection system, counterstained with Cresyl violet. (right) Schematic picture of the olfactory bulb. The cross indicates the approximate injection position in the left picture. ONL, olfactory nerve layer; GL, glomerular layer; EPL, external plexiform layer; GCL, granule cell layer. (d-f) Amount of time (s) that rats investigate stimulus rats in the sampling phase and in the discrimination phase (known or novel rat) following microinjection (1 µL per bulb) with only vehicle (d), atropine (1 µg/ 1 µL) and vehicle (e) or atropine and VP (1 ng/ 1 µL, f). Data are presented as box-plots including median and distribution of single data points. Paired Samples t-Test between known and novel, *$p<0.05$, n=13 (Veh/Veh), n=14 (Atr/Veh), n=14 (Atr/VP).

363 **Discussion**

364 **Is bulbar VPC activity increased during social interaction?**

365

366 Social discrimination in rats depends on the presence of endogenous VP in the OB [7], which
367 implies that social interaction can trigger VP release, via the activation of bulbar VPCs. A
368 substantial background activity of VPCs (pERK) was found throughout all stimulation groups
369 *in-vivo*, even though VPCs are inhibited by olfactory nerve input *in-vitro*. This background
370 activity might be related to the circumstance that it is not realistic to deprive our experimental
371 rats from all environmental sensory inputs, e.g., rat odors from other cages [40]. Nevertheless,
372 we observed increased levels of bulbar VPC activation during social interaction (Fig. 1c+d).
373 Thus, our results suggest that during social interaction VPC activity and hence the probability
374 of bulbar VP release, are substantially increased. This finding is apparently at variance with
375 others from Wacker et al. [41], who reported that social interaction cannot trigger the expression
376 of the immediate early genes c-Fos or Egr-1 in bulbar VPCs. However, as discussed by them,
377 a missing expression signal of those genes might be explained by their general absence of
378 expression in bulbar VPCs.
379 Since we know that VPCs are primarily inhibited by ON inputs *in-vitro* [8], we hypothesized that
380 additional inputs from outside of the OB are responsible for the activation of VPCs during social
381 interaction.

382

383 **Can Pheromones modulate bulbar VPCs during social odor perception?**

384

385 Pheromones from conspecifics are detected by rodents during social interactions and were
386 shown to directly influence social behaviors, such as sexual behavior or aggression between
387 conspecifics [42, 43]. Thus, pheromones would be an obvious way to provide social specificity via
388 social interactions. Indeed, M/TCs in the AOB, the first pheromonal relay station in the brain,
389 are known to innervate the dorsal MOB and therewith could also excite bulbar VPCs [24]. In our
390 hands, electric stimulation of the AOB failed to elicit any excitatory responses in MOB VPCs in

391 *in-vitro* sagittal slice experiments (Supplemental Fig. 2d+e). Moreover, there was no
392 significantly enhanced MOB VPC activation by urine, containing pheromones, compared to
393 control. However, we cannot entirely rule out this possibility because of the reduced
394 connectivity *in-vitro* and the larger/different set of pheromonal cues accessible during
395 investigation of a conspecific versus just urine. Moreover, although social interaction increases
396 c-Fos expression in the AOB in general [25], we did not find any differences in the number of
397 pERK$^+$ AOB M/TCs between the rat, urine, and water exposure group (Supplemental Fig. 1c+f).
398 Also, we rarely observed pERK$^+$ VPCs in the AOB itself, neither following urine exposure nor
399 social interaction (only 1 or even less cells on average per slice). In summary, pheromonal
400 AOB signaling is rather unlikely to underlie VP-dependent individual social discrimination in
401 the MOB.
402 Also, while removal of the vomeronasal organ initially prevents social recognition of same sex
403 individuals, it is reinstated after 14 days, indicating that AOB functioning is not required for
404 social recognition *per se* [21]. Nevertheless, the AOB is crucial for individual discrimination in the
405 context of reproduction. For example, the pheromonal memory of the stud male in female mice
406 results in a pregnancy block induced by odors of male strangers. This consequence of social
407 odor recognition, known as the Bruce effect, depends on pheromonal processing in the AOB
408 [44]. Thus, the AOB may be essential for individual discrimination in certain situations, such as
409 in a reproductive context, but not necessarily in social discrimination in general. Still, it is
410 possible that modulatory top-down inputs to the MOB that are activated by AOB processing [45]
411 is involved in the activation of MOB VPCs.
412
413 **How does ACh modulate VPC activity?**
414
415 Cholinergic neurons in the HDB are the only known source that provides centrifugal
416 neuromodulatory inputs to the GL of the OB, where VPCs are predominantly located [8, 29, 30].
417 Following social interaction, the number of pERK$^+$ cholinergic HDB neurons was significantly
418 higher compared to rat urine exposure (Fig. 5c) indicating that cholinergic activation might be

419 involved in bulbar VPC activation in the rat exposure group (Fig. 1c). Accordingly, we observed
420 that ON-evoked IPSPs are reversed into EPSPs/APs in 75 % of examined VPCs during ACh
421 administration *in-vitro* (Fig. 2g). Moreover, we showed that ACh induces both, reduced
422 inhibition, and stronger ON-driven excitation (Fig. 3a-d). Reduced GABAergic inhibition by ACh
423 was already observed in hypothalamic VPCs, resulting in increased VP release *in-vitro* [46, 47].
424 Non ACh-specific optogenetic silencing of all vesicular release from HDB projections in the OB
425 reduces glomerular responses to odor stimulation *in-vivo* [30]. In addition, optogenetic
426 stimulation of specifically HDB cholinergic projections in the OB *in-vivo* increases odor
427 responses in projection neurons [37, 38]. Both results indicate overall excitatory effects of HDB
428 cholinergic modulation in the OB during odor stimulation. Cells in the GL were reported to have
429 a particularly high sensitivity for ACh, and direct application of ACh resulted in both, increase
430 and decrease of spontaneous spiking rates in individual cells there [48]. These bidirectional
431 effects may be explained by the presence of two different ACh receptor subtypes, nicotinic and
432 muscarinic receptors, and their distinct effects on the various cell types of the OB [49].
433 In our experiments, we demonstrated that muscarinic stimulation with either muscarine or
434 mecamylamine-ACh application reversed evoked inhibition into excitation in some VPCs (Fig.
435 4e-h). At the level of the GL, it was shown that the muscarinic pathway enhances inhibitory
436 inputs to GABAergic interneurons, i.e., periglomerular cells and short axon cells, hence
437 possibly causing disinhibition of VPCs [26]. According to our data, mainly muscarinic but not
438 nicotinic stimulation reduced ON-evoked IPSP amplitudes in VPCs (Fig. 4a-h). In line with our
439 observation, *in-vivo* Ca^{2+} imaging revealed that muscarinic stimulation increases glomerular
440 sensitivity to odor presentation [50].
441 All our pharmacological manipulations *in-vitro* were performed via bath application. Since
442 nicotinic receptors are ionotropic and known to get desensitized [51], locally and temporally more
443 precise administration, such as puff application or optical uncaging, may be informative to
444 investigate nicotinic mechanisms on a single cell level. Indeed, although we observed no
445 statistical differences in nicotine effects on evoked-IPSP amplitudes, increasing and
446 decreasing effects of nicotine application could be found across individual VPCs (Fig. 4a+b).

447 In this context, D'Souza and Vijayaraghavan [52] described that nicotinic receptor signaling is
448 involved in gain control mechanisms of excitatory projection neurons in the OB, which might
449 explain the variable effects that we observed upon nicotine and atropine-ACh application.
450 Moreover, muscarine application did not entirely replicate ACh effects (Fig. 2g, Fig. 4f+h). Thus,
451 we cannot fully exclude nicotinic action in modulation of VPCs. Furthermore, the origin of the
452 ON-driven excitation that is responsible for triggering APs during ACh application still needs to
453 be identified. Possible candidates would be neurons providing somatic and lateral dendritic
454 inputs to VPCs since ON-evoked Ca^{2+} signals in the tuft were not increased in ACh (Fig. 3g).
455 Although here we focused on the cholinergic system because of the strength of cholinergic
456 effects, our *in-vitro* electrophysiology results indicate that increased VPC excitability could be
457 triggered by synergistic cholinergic, serotonergic, and noradrenergic modulation; the possibility
458 of such cooperative action should be accounted for in future studies.
459
460 **How is the ACh system activated in the context of social interaction?**
461
462 If centrifugal cholinergic modulation from the HDB is indeed responsible for increasing VPC
463 activity, the question remains how ACh is released in the OB in a context-dependent manner
464 such as social interaction. Social perception is thought to be a multisensory process as diverse
465 inputs from the whole stimulus animal are sampled and integrated [4, 10, 53]. In support of this
466 idea, Matsuo et al. [3] showed that genetic ablation of dorsal MOB glomeruli impairs the expected
467 emission of ultrasonic vocalization by male mice towards female urine, whereas these mice
468 still emit ultrasonic vocalizations in the presence of a whole female mouse. This indicates that
469 other sensory stimuli than those provided by olfaction can trigger this social behavior.
470 Moreover, it was shown that rats, which were exposed to just volatile odors of stimulus rats
471 during the social discrimination paradigm cannot discriminate the different sources of these
472 odors [25]. According to our hypothesis, this impairment might be due to the absence of non-
473 olfactory cues and lack of arousal.

474 Intriguingly, the HDB or the ACh system in general is activated by various sensations, such as
475 olfactory, visual, and tactile stimuli [31, 32, 36]. Stimulation of the HDB cholinergic projections or
476 ACh application in turn can enhance as well as reduce neural activity in all primary sensory
477 cortices [54, 55, 56]. Also, especially if the sensation is associated with learning, ACh tends to be
478 released in the respective sensory cortex, for example during conditioning of auditory or tactile
479 cues with food as an unconditioned stimulus [36, 57]. Accordingly, our data demonstrates
480 substantial HDB ACh activity during social interaction. Surprisingly, we were not able to find a
481 significant difference between water stimulation and social interaction in ACh neurons of the
482 HDB. It is not possible to determine from our data what may be the reason for this high
483 activation in the water condition. However, water stimulation (with no or few olfactory cues)
484 was not enough to increase pERK activity in MOB VPCs to the same level as social interaction,
485 suggesting that both, ACh neuron activation in the HDB and olfactory inputs are needed for
486 VPC activation. In support, our *in-vitro* electrophysiology results demonstrate that ACh
487 modulation promotes especially excitation in VPCs following ON stimulation mimicking odor
488 stimulation. Thus, it is tempting to speculate that the HDB cholinergic system could play a role
489 as a multisensory integration center during complex contexts like social interaction that
490 provides modulatory feedback to sensory processing, including but not limited to olfaction.
491 Intriguingly, similar multi-sensory integration is also discussed to take place in the insular
492 cortex which is responsible for coordinated behavioral output during social decision-making [58].
493 From a translational point of view, it is interesting to note that also human research on social
494 behavior deficits suggests a social-context network that integrates social cues (frontal lobe),
495 consolidates social-context associations (temporal lobe), and converges environmental and
496 internal signals (insular lobe) [59].
497 Moreover, ACh activity correlates with certain internal states in animals, e.g., arousal or
498 attention [33, 34, 35]. This internal state-dependent ACh release is triggered by the sudden
499 presence or novelty of stimuli [16, 60]. Rats discriminate individuals according to their social
500 novelty [4]. Thus, we suggest that both multi-sensation and increased arousal and attention while

assessing the novelty of rats in the context of social interaction can lead to increased HDB ACh activity and thereby cholinergic neurotransmission in the OB.

Why is ACh-dependent VP neurotransmission involved in social discrimination?

Our pERK and electrophysiological experiments imply a central role for ACh in VP-dependent social discrimination and accordingly social memory. The involvement of centrifugal ACh as a facilitator of olfactory learning or habituation has been investigated for decades [61]. The blockade of the muscarinic pathway in the OB impairs both aversive and appetitive learning [62, 63]. Intriguingly, it was shown that the blockade of muscarinic neurotransmission in the OB by scopolamine does not impair single-molecule odor recognition [64]. However, non-ACh specific optogenetic silencing of overall release from HDB projections in the OB impairs social habituation to female conspecific mice [30]. In addition, here we demonstrated that the injection of the muscarinic antagonist atropine in the OB efficiently blocks the recognition of a known rat in the social discrimination task. These findings indicate that social discrimination/habituation paradigms and simple odor discrimination/habituation paradigms differ from each other.

Regarding sensory complexity, social discrimination recruits multiple senses, whereas odor discrimination is limited to mostly mono-molecular odorants. As mentioned above, multisensory stimulation is a known trigger for the activation of HDB ACh neurons. Atropine-induced impairment of social discrimination was rescued by additional VP injection in the OB (Fig. 6f). Therefore, we suggest that ACh facilitates social discrimination via enhancing bulbar VP release. Since bulbar VP signaling is essential for multisensory social discrimination but not for simple odor habituation [7], we suggest that the probability of bulbar VP release is higher during social discrimination. This hypothesis is supported by a study with another social behavior-related neuropeptide, oxytocin, in which Martinon et al. [65] demonstrated that oxytocin release in the bed nucleus of stria terminalis is not increased with a foot shock alone, but when the foot shock is paired with another sensory cue (condition stimulus). Intriguingly,

529 multisensory integration was recently also implied in a context of social discrimination.
530 Accordingly, rats and mice cannot recognize their cage mates if they are immobile due to
531 anesthesia, and mice that are both whiskerless and deaf are not able to discriminate awake
532 novel and known conspecifics anymore [66].
533 We showed that social interaction as well as ACh activate bulbar VPCs, indicating that
534 cholinergic activation contributes to increased activation of the bulbar VP system during social
535 interaction. However, the pERK results also indicate that the entire neuronal population of the
536 bulb shows increased activation, not just VPC neurons, upon social exposure. Thus,
537 alternatively to a multisensory driven specific activation of bulbar VPCs, it is possible that a
538 general arousal mechanism leads to an increased excitation of the entire bulbar network,
539 including VPCs. Accordingly, this might also explain to a certain degree why urine, in contrast
540 to a rat stimulus, did not activate significantly more VPCs than water, since urine might cause
541 less general arousal than a hitherto unknown conspecific.
542 The absence of sensitivity to both, the muscarinic antagonist or a V1a receptor knock-down by
543 siRNA in simple odor discrimination and habituation [7, 64] implies that ACh-induced VP signaling
544 is only necessary to differentiate difficult odor mixtures. Interestingly, ACh was reported to play
545 a critical role in modulating olfactory perceptual learning tasks [61]. Perceptual learning is a
546 prerequisite for enhanced perceptual acuity during discrimination of previously experienced
547 stimuli. Like social discrimination, perceptual learning is specific for trained stimuli (e.g., a
548 conditioned odor, a previously sampled rat) and requires a certain attention/arousal of the
549 learning animal. This enhancement of olfactory acuity is mediated by muscarinic signaling [61].
550 Thus, ACh-dependent VP neurotransmission might be involved not only in social discrimination,
551 but also olfactory perceptual learning tasks in general, e.g., discrimination of closely related
552 odor mixtures. Indeed, different body odors should be difficult to discriminate due to their
553 complexity and similarity. Singer et al. [67] showed that volatile MHC components in mouse urine
554 contain similar compositions of compounds across strains suggesting that volatile MHCs are
555 not distinguishable by the presence or absence of some unique compounds. However, the
556 amplitudes of some prominent compound peaks in the gas chromatogram are different

557 between strains, indicating that mice can recognize the differences of relative concentrations
558 of certain compounds in body odor mixtures. Rats perceive not only volatile urinary odors but
559 also volatile odors from other sources and even differentiate individuals from the same strain
560 during the social discrimination task. Thus, it is likely that the olfactory cues that they can
561 discriminate are even more complex. We therefore suggest that additional bulbar VP
562 neuromodulation is needed to enhance the signal-to-noise ratio of complex odor inputs to allow
563 better identification of individual body odors. Reduced activity of individual projection neurons
564 via increased activity of interneurons is thought to act as a filtering mechanism [68, 69].
565 Although social interaction increased pERK activation in MCs (Fig. 1e), inhibition of pERK^{+}
566 MCs, e.g., via a reduction of their firing frequency could still take place. E.g., pERK signaling
567 could be not sensitive or fast enough to register this inhibition or pERK signaling is just
568 gradually decreased but still higher than during baseline activity. Indeed, it was already shown
569 that VP administration dampens odor-evoked firing of MCs in anesthetized rats [7] and reduces
570 ON-evoked EPSPs in external tufted cells *in-vitro* [8]. Thus, we suggest that this filtering effect
571 facilitated by bulbar VP can further reduce weak or quantitatively similar inputs, so that only
572 quantitatively prominent inputs are transmitted to higher brain regions leading to more
573 prominent differences in the neuronal representation of different social odor signatures. This
574 reduction of noise could help the rats to discriminate similar mixtures of body odors during the
575 social discrimination task, but also during social interaction in nature.

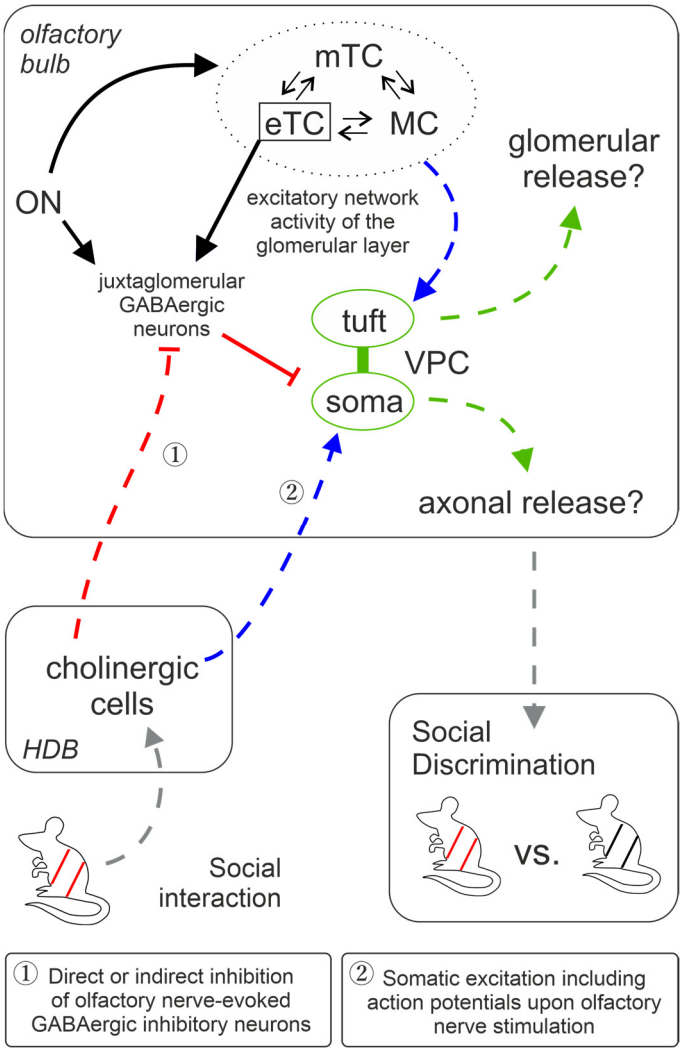

Fig. 7. Graphic summary of olfactory bulb pathways involved in social discrimination

Blue, green, and grey arrows represent excitatory and red lines inhibitory pathways indicated by this study and our previous publication [8]. The cells within the dashed circle indicate the excitatory network within the same home glomerulus. Dashed pathways were confirmed but not fully dissected on the synaptic level. Green pathways are related to vasopressin signaling, grey pathways to sensory input or behavioral output and black pathways are based on findings from literature. Question marks indicate potential dendritic and axonal release of VP in the OB. Axonal projections innervate GL, EPL, MCL, and sGCL. EPL, external plexiform layer; eTC, external tufted cell; GL, glomerular layer; HDB, horizontal limb of the diagonal band of broca; MC, mitral cell; MCL, mitral cell layer; mTC, middle tufted cell; ON, olfactory nerve; sGCL, superficial granule cell layer; VPC, vasopressin cell.

587 **Methods**

588 **Animals**

589

590 All experiments were conducted according to national and institutional guidelines for the care
591 and use of laboratory animals, the rules laid down by the EC Council Directive (86/89/ECC),
592 German animal welfare and the local government of Oberpfalz and Unterfranken. Wistar rats
593 of either sex were purchased from Charles River Laboratories (Sulzfeld, Germany) or bred
594 onsite in the animal facilities at the University of Regensburg. Heterozygous VP-eGFP Wistar
595 rats [20] of either sex were bred at the University of Regensburg. The light in the rooms was set
596 to an automatic 12 h-cycle (lights on 07:00-19:00).

597

598 ***In-vivo* social stimuli exposure experiment**

599 **Stimuli exposure**

600

601 Three cohorts of male VP-eGFP rats (5-6 weeks) were single-housed at least 3 hours before
602 the experiment for habituation to the new environment. Stimuli used were water, juvenile rat
603 urine (collected and mixed from at least 3 juvenile male, stimulus rats) and juvenile rats (3-4
604 weeks, male non-cage mates). Water and urine (both 50 µl) were applied on filter papers (2
605 cm x 3 cm). The different stimuli were gently introduced in the cage and the rats could explore
606 freely. A stimulus exposure lasts 4 min in which the behavior of the rats was video-taped for
607 confirmation of proper stimulus sampling. Rats that did not directly sniff at the filter paper
608 containing water or urine as well as rats that did not perform proper social investigation (sniffing
609 anogenital and head region, for details see Video analysis: Social investigation) were excluded
610 from the experiment. Immediately after the exposure, rats were deeply anesthetized for
611 transcardiac perfusion and fixation of the brain.

612

613 **Transcardiac perfusion**

614

615 Rats were deeply anesthetized with an i.p. injection of ketamine-xylazine (100 mg/kg and 10
616 mg/kg, respectively). The abdomen and the diaphragm were incised to expose the thoracic
617 cavity. After opening the mediastinum, a needle was inserted into the left ventricle. Following
618 incision of the right atrium, 0.1 M PBS pH 7.4 was perfused for 4 min with a speed of 9.5
619 mL/min by a pump (GZ-07528-30, Cole-Parmer, Wertheim, Germany) followed by 4 % PFA-
620 PBS for 4 min. Rats were decapitated and the whole brains were extracted. Brains were post-
621 fixed in 4 % PFA-PBS overnight at 4 °C and stored in 30 % sucrose-0.1 M PB at 4 °C for at
622 least 2 days then kept at 4 °C until slicing.
623
624 **Immunohistochemistry**
625
626 Brains were sliced with a cryostat (CM3050 S, LEICA, Wetzlar, Germany) at approx. -20 °C,
627 then stored in cryoprotectant solution (0.1 M phosphate buffer, 500 mL; Ethylene Glycol, 300
628 mL; Sucrose, 300 g; Polyvinyl-pyrrolidone, 10 g) at -20 °C until staining. The OB was cut
629 horizontally with a thickness of 30 µm. On average, six slices from one bulb of each
630 experimental rat were used for staining. The HDB (Figure 24-28 (1.08 - 0.60 mm from the
631 Bregma) in the rat brain atlas [70]) was cut coronally with a thickness of 30 µm. Three slices of
632 each experimental rat were used for staining.
633 All immunohistochemistry procedures were performed in 12 well plates (Corning Incorporated,
634 Corning, NY, USA) with the free-floating method. Slices were washed three times with 0.3 %
635 Triton-X100 in PBS (PBST) for 10 minutes. Then slices were incubated in methanol for 10
636 minutes at -20 °C. After washing with PBST for 10 minutes, incubation with 0.1 M Glycine in
637 PBS was performed for 20 minutes at room temperature, followed by washing with PBST for
638 10 minutes. Slices were incubated with the blocking solution for one hour at room temperature.
639 The blocking solution contained 0.2 % of cold water fish skin gelatin (AURION, Wegeningen,
640 Netherlands) and 0.01 % of NaN3 in normal donkey serum (NB-23-00183-1, NeoBiotech,
641 Nanterre, France). Incubation with primary antibodies (see Antibodies) diluted in the blocking
642 solution was carried out for 72 hours at 4 °C. After washing three times with PBST for 10

643 minutes, secondary antibodies diluted in the blocking solution were added and incubated for
644 two hours at room temperature, followed by washing three times with PBST for 10 minutes.
645 From the incubation in secondary antibodies on, every procedure was performed in the dark
646 to avoid bleaching fluorescence. For choline acetyltransferase (ChAT) staining, the protocol
647 was modified. Additional blocking by incubation with avidin and biotin (both 0.001% in PB,
648 Sigma-Aldrich, Darmstadt, Germany) for 30 min and a 10 min wash with PBST in between
649 were carried out before incubation with the blocking solution. Moreover, after the last washing
650 with PBST, incubation in streptavidin conjugated with CF488 (1:400 in PBST, #29034, Biotium,
651 Fremont, CA, USA) for two hours at room temperature was carried out. After staining itself,
652 slices were washed three times with PBST for 10 min. Slices were mounted on objective slides
653 (Thermo Fisher Scientific, Waltham, MA, USA) using DAPI fluoro mount-G (Southern Biotech,
654 Birmingham, AL, USA).
655
656 **Antibodies**
657
658 Primary antibodies were goat anti-GFP (1:1000, #600-101-215S, Rockland, Limerick, PA,
659 USA), Rabbit anti-P-p44/42 MAPK (1:1000, #9101S, Cell Signaling Technology, Frankfurt am
660 Main, Germany), Sheep Anti-Choline Acetyltransferase (1:125, ab18736, Abcam, Berlin,
661 Germany). Secondary antibodies were Donkey anti-Goat IgG conjugated with CF488 (for GFP,
662 1:1000, #20016-1, Biotium), Donkey anti-Rabbit IgG conjugated with CF594 (for pERK, 1:1000
663 for the OB and 1:500 for the HDB, #20152, Biotium), biotinylated Donkey anti-Sheep IgG (for
664 ChAT, 1:250, #20191-1, Biotium). All antibodies were diluted in the blocking solution.
665
666 **Fluorescent Microscopy**
667
668 Fluorescent images of the stained slices were obtained using a DM6 B microscope (LEICA)
669 and the software, LAS X (LEICA). DAPI, CF488 and CF633 were stimulated with an exposure
670 time of 300 ms, 300 ms and 500 ms, respectively. Tile-stitching and z-stack of pictures were

671 performed by LAS X. After taking pictures, those were processed by 3D deconvolution or the
672 Lightning & Thunder process (LAS X) to improve the contrast. Pictures were converted to .tif
673 files using Fiji (ImageJ, downloaded from https://imagej.net/Fiji/Downloads) and contrast was
674 adjusted to the same levels in every picture. Z-stack pictures from approx. 5-6 different z-
675 positions per bulb or rats were used for analysis.
676
677 **Cell counting**
678
679 Immunoreactive cells were counted manually using the multi-point tool or cell counter plug-in
680 in Fiji. 4-6 OB slices and 2 HDB slices were analyzed. Double positive cells were identified by
681 comparing two color channels. The position of counted cells was saved as .roi files or .xml files.
682 The number of cells was averaged per experimental rat and bulb. The counting was done in 4-
683 6 non-overlapping sections of one olfactory bulb of a respective rat. The total number of
684 positive cells was averaged over the number of counted sections, to account for variance in
685 cell distribution and number of sections analyzed. In the OB double-labelled cells were counted,
686 if the typical soma shape was visible without a staining of the nucleus area in the GFP-channel
687 (green) and could be identified with the same outline in the pERK channel (magenta, see
688 example in Fig. 1a). In the HDB double-labelled cells were counted, if the typical soma shape
689 was visible in the pERK-channel (magenta) and could be identified with the same outline in the
690 ChAT-channel (green, see example in Fig. 5a). For control the localization of the nucleus was
691 double-checked in the DAPI channel (blue).
692 All the data was analyzed by an observer blinded with respect to stimulation groups.
693
694 **Electrophysiology**
695 **Slice preparation**
696
697 11-18 day-old juvenile VP-eGFP rats were used for *in vitro* electrophysiology experiments. The
698 rats were deeply anesthetized with isoflurane and quickly decapitated. Horizontal and sagittal

699 slices (300 µm) were cut in ice-cold carbogenized ACSF (artificial cerebrospinal fluid; mM: 125
700 NaCl, 26 NaHCO3, 1.25 NaH2PO4, 20 glucose, 2.5 KCl, 1 MgCl2, and 2 CaCl2) using a
701 vibratome (VT 1200, LEICA) and afterwards incubated in ACSF at 36 °C for 45 min. Until
702 experiments, the slices were kept at room temperature (approx. 21°C) in ACSF.
703
704 **Electrophysiology**
705
706 Brain slices were placed in a recording chamber on the microscope's stage perfused with
707 carbogenized ASCF circulated by a perfusion pump (ISM 850, Cole-Parmer). GFP-labeled
708 vasopressin cells (VPCs) were identified with LED illumination (470 nm) under a modified Zeiss
709 Axioplan microscope (Carl Zeiss Microscopy, Oberkochen, Germany). Epifluorescence was
710 filtered by a long-pass dichroic mirror (490 nm cutoff) and an emission filter (510 ± 21 nm) and
711 visualized with a digital camera (VisiCAM-100, Visitron Systems, Puchheim, Germany). To
712 perform whole-cell patch-clamp recordings, cells were visualized by infrared gradient-contrast
713 illumination via IR filter (Hoya, Tokyo, Japan). Glass pipettes for recordings were pulled by a
714 pipette puller (Narishige, Tokyo, Japan) sized 4-6 MΩ and filled with intracellular solution (in
715 mM: 130 K-methylsulfate, 10 HEPES, 4 MgCl2, 4 Na2ATP, 0.4 NaGTP, 10 Na
716 Phosphocreatine, 2 ascorbate, pH 7.2). Recordings were performed with the current-clamp
717 configuration using an EPC-10 (HEKA, Lambrecht, Germany) digital oscilloscope. Series
718 resistance was measured 10-30 MΩ. The average resting membrane potential was -50 to -60
719 mV. Experiments were only started in case the patched cells had a holding current below ~ -
720 50 pA and no drastic drift in the resting membrane potential.. Experiments were performed at
721 room temperature (approx. 21°C).
722 In experiments with AOB stimulation, sagittal slices including the accessory olfactory bulb
723 (AOB) were used. VPCs for these experiments were identified in the posterior-dorsal area of
724 the MOB (Supplemental Fig. 2c) since intact projections of AOB mitral/tufted cells to this area
725 in sagittal slices were demonstrated using antidromic electrical stimulation previously [24]. Glass

726 pipettes, intracellular solution and settings of oscilloscope were same as experiments with
727 horizontal slices.
728
729 **Electrical extracellular stimulation**
730
731 Olfactory nerve (ON) stimulation was performed with a glass pipette stimulation electrode sized
732 around 2 MΩ. Glass pipettes were filled with ACSF. The electrode was connected to an
733 external stimulator (STG 1004, Multi-Channel Systems, Reutlingen, Germany) controlled by a
734 PC. The stimulation strength was adjusted with the stimulator's software (MC_Stimulus, V
735 2.1.5) and stimulation was triggered by the amplifier software (Patchmaster, HEKA).
736 Stimulation pipettes were gently placed in the ON layer anterior to a cell to patch using a
737 manual manipulator (LBM-7, Scientifica, East Sussex, UK) under optical control with the
738 microscope. The stimulation strength was 50-400 µA for 100 µs. The stimulation was triggered
739 every 30 s to avoid desensitization of the neural networks.
740 AOB stimulation was performed with a glass pipette stimulation electrode; the stimulator and
741 the software were the same as for MOB ON stimulation. Stimulation pipettes were gently
742 placed in the vomeronasal nerve layer or in the EPL/mitral cell layer in the AOB using a manual
743 manipulator (LBM-7, Scientifica, East Sussex, UK) under optical control with the microscope.
744 The stimulation strength was 50-500 µA for 100 µs.
745
746 **Ca^{2+} Imaging**
747
748 Fluorescence was recorded by two-photon laser scanning microscopy on a Femto-2D
749 microscope (Femtonics, Budapest, Hungary), equipped with a tunable, Verdi-pumped Ti:Sa
750 laser (Chameleon Ultra I, Coherent, Glasgow, Scotland). The microscope was equipped with
751 a 60x Nikon Fluor water-immersion objective (NA 1.0; Nikon Instruments, Melville, NY, USA),
752 three detection channels (green fluorescence (epi and trans), red (epi) and infrared light
753 (trans)) and controlled by MES v4.5.613 software (Femtonics).

754 VP-eGFP cells were identified in the green channel at an excitation wavelength of 950 nm.
755 VPC bodies were patched in the whole-cell mode with patch pipettes filled with regular
756 intracellular solution (see Electrophysiology), Alexa Fluor 549 (50 µM, Invitrogen) and the Ca^{2+}
757 indicator OGB-1 (100 µM, Invitrogen, Thermo Fisher Scientific) were added for neurite
758 visualization and Ca^{2+} imaging. Fluorescence transients and image stacks were acquired at
759 800 nm laser excitation. Data were mostly collected from the medial surface of the OB. Ca^{2+}
760 imaging experiments were performed at room temperature (approx. 21° C). The patched VPCs
761 were held in the current clamp mode near their resting potential of -55 mV. Structures of
762 interest were imaged in free line-scanning mode with a temporal resolution of approx. 1 ms.
763
764 **Experimental design and data analysis**
765
766 All drugs (see Pharmacology) diluted in ASCF were bath-applied via the perfusion system.
767 Recordings under pharmacology were performed at least 5 min after the onset of
768 administration to ensure that the drugs reached the recorded cell. Two average traces from 3-
769 5 recordings in each condition were analyzed. The data was averaged per condition. The
770 amplitudes of PSPs were measured using Origin 2018b (Origin Lab). The amplitudes of IPSPs
771 following pharmacology were normalized to the amplitudes during the ACSF condition (100 %).
772 The amplitudes of EPSPs following bicuculline application with pharmacology were normalized
773 to the amplitudes during the bicuculline condition (100%). APs, EPSPs, IPSPs in experiments
774 with ACh application were defined as: APs, the existence of AP (s) after ON stimulation; EPSPs,
775 observation of depolarization with amplitudes of >1.5 mV; IPSPs, the absence of APs and
776 EPSPs. In some experiments with ACh, current (40, 60, 80, 100 pA, 600 ms) was injected via
777 the recording electrode into the cell to test if ACh application alters the intrinsic excitability in
778 VPCs. Spiking rates of AP trains were calculated as the number of spikes divided by the
779 duration of AP trains. Latency of the first spike was measured as the duration between the
780 current injection onset and the peak of the first spike.

781 In some experiments, simultaneous to the electrophysiological recordings, intracellular Ca^{2+}
782 transients were measured at the tuft and at the apical dendrite directly apical to the soma (see
783 Ca^{2+} Imaging) following ON stimulation. Three consecutive focal line-scans were performed
784 during ON stimulation (see Olfactory nerve stimulation). To confirm that the cell was correctly
785 filled with Ca^{2+}-dye, VPCs were also stimulated with somatic 50 Hz trains (20 APs) via the
786 patch pipette which was shown to reliably trigger Ca^{2+} Influx in case ON stimulation did not
787 result in Ca^{2+} signals near the soma during olfactory nerve stimulation [8]. The three line scans
788 per pharmacological condition were averaged for analysis. Dendritic Ca^{2+} transients were
789 analyzed in terms of $\Delta F/F$ relative to the resting fluorescence F_0 [71]. The time course of
790 pharmacology and analysis were the same as for electrophysiological data mentioned above.
791 All the data was analyzed by an observer blinded with respect to pharmacology.
792
793 **Pharmacology**
794
795 All pharmacological agents used were diluted in ACSF for bath application: serotonin
796 hydrochloride (20 µM, Sigma-Aldrich), DL-Norepinephrine hydrochloride (20 µM, Sigma-
797 Aldrich), acetylcholine chloride (100 µM, Sigma-Aldrich), mecamylamine hydrochloride (20 µM,
798 Sigma-Aldrich), atropine (10 µM, Sigma-Aldrich), (-)-Nicotine, Ditartrate (100 µM, Merck KGaA,
799 Darmstadt, Germany), (+)-Muscarine chloride (1µM, Sigma-Aldrich), 1(S),9(R)-(-)-bicuculline
800 methyl bromide (50 µM, Sigma-Aldrich).
801 The doses used were chosen based on minimal doses reported to elicit *in-vitro* effects [8, 26, 47,
802 72, 73, 74, 75, 76].
803
804 **Behavioral Pharmacology**
805 **Cannula implantation**
806
807 Three cohorts of 5-6 week-old male Wistar rats were group-housed until surgery. To allow local
808 injection of pharmacological solutions in the OB without anesthesia, we bilaterally implanted

809 guide cannulae (23 G, Injecta GmbH, Klingenthal, Germany) in the rat OB. Before surgery, all
810 surgical instruments were autoclaved at 121 °C for 20 min. The rats were anesthetized by
811 isoflurane using a TEC 3 isoflurane vaporizer (Eickemeyer, Tuttlingen, Germany). The
812 concentration of isoflurane was maintained between 2-3 %. The rats were fixed on a
813 stereotaxic frame (TSE, Bad Homburg Germany/Kopf, Tujunga, CA, USA) using ear bars. To
814 prevent hypothermia, the rats were kept warm using a warming pad (ThermoLux, Witte + Sutor,
815 Murrhardt, Germany). Analgetics (buprenorphine, 0.1 mg/kg s.c., Bayer, Beline, Germany) and
816 antibiotics (enrofloxacin, 10 mg/kg s.c., Bayer) were injected before surgery. After shaving the
817 head and disinfection of the operation site with 70 % ethanol, we incised the scalp and the
818 supporting tissue on the skull. Injection of lidocaine hydrochloride (2 %, around 100 µL, bela-
819 pharm, Vechta, Germany) under the scalp was operated if needed. Two stainless steel
820 jeweler's screws were inserted into the skull using a surgical drill (NM 3000, NOUVAG,
821 Goldach, Switzerland). One on the left anterior to bregma and the other one on the right
822 posterior to bregma to secure dental cement fixation. Holes for guide cannulae were made by
823 a drill, followed by placement of cannulae 7 mm anterior and 1.2 mm lateral relative to bregma
824 as well as 1 mm ventral from the surface of the skull where 2 mm above the injection
825 coordinates. Thus, the coordinates for injection were 3 mm ventral to the surface of the skull
826 [70]. Cannulae and the two screws were fixed together by the dental cement (Kallocryl, Speiko-
827 Dr. Speier GmbH, Muenster, Germany). Once the cement dried, the connection between the
828 cement and the scalp was disinfected by iodine solution and cannulae were blocked by
829 insertion of stainless steel stylets (25 G, BD, Heidelberg, Germany) to prevent dust entering
830 the cannulae that could result in infection or blockage. The rats were removed from the frame
831 and placed in fresh cages for recovering from anesthesia under observation until they are
832 awake. The rats were weighed prior to surgery and on the next day to see if they recovered
833 properly after surgery. Their health condition and behavior were checked for at least five days.
834 After surgery, they were single-housed until experiments to prevent damage to the guide
835 cannulae. Meanwhile, the rats were handled and habituated to the removal and insertion of

836 stylets every day until experiments. Stylets were cleaned with 70 % ethanol every time they
837 were removed from the guide cannula.
838
839 **Social discrimination with pharmacology**
840
841 We combined the social discrimination paradigm [4] and microinjection of pharmacology into the
842 OB. The social discrimination paradigm consists of a sampling phase and a discrimination
843 phase. Experiments were performed in the afternoon. In the sampling phase (4 min), one
844 stimulus rat was gently introduced into the cage of the experimental rats. Then the stimulus rat
845 was removed from the cage and the experimental rat stayed in the cage alone for an inter-
846 exposure interval of 30 min. In the discrimination phase (4 min), two stimulus rats, one is the
847 same as during the sampling phase and the other one is a novel stimulus rat, were gently
848 introduced into the cage. During both phases, the behavior of the experimental rat was video-
849 taped from above through a transparent plastic plate for post-hoc analysis. Stimuli were 3-4
850 week-old group-housed male rats that were single-housed only in between the social
851 exposures of the behavioral experiments to prevent mixing of body odors. They were marked
852 with a red or black pen of the same brand (Edding, Ahrensburg, Germany) to allow visual
853 differentiation by the observers. Pharmacological agents diluted in ACSF include atropine (1
854 µg in 1 µL) and [Arg8]-vasopressin acetate salt (1 ng in 1 µL, Sigma-Aldrich). 40 min before
855 the sampling phase, either ACSF or atropine was injected into both OB hemispheres (1 µL
856 each). 10 min before the sampling phase, either ACSF or VP was injected into both OB
857 hemispheres (1 µL each). All injections were carried out with microinjection syringes (Hamilton,
858 Bonaduz, Switzerland) connected to a self-made injection system which consists of plastic
859 tubes and 10 mm-long 30 G needles (2 mm longer than the guide cannulae). After every
860 injection (1 µL), the injection systems rested in place for 1 min to allow the injected solution to
861 diffuse fully in the tissue. The doses used were chosen based on minimal does reported to
862 elicit behavioral effects [6, 77]. No anatomical outliers in stereotaxic cannula implantation had to
863 be excluded from behavioral analysis (Fig. 5). However, one animal from the control group was

removed, as it showed a high amount of unspecific sexual/mounting behavior towards the stimulus animals throughout the sampling as well as the discrimination phase. To confirm that neither atropine nor VP microinjection into the OB induced unspecific behavioral effects, we demonstrated that these manipulations did not interfere with non-social investigatory/play behavior and habituation (towards amyl acetate (Sigma-Aldrich)/ (-)-carvone (Sigma-Aldrich) presented in a teaball or a juvenile rat) during the sampling phase (Supplemental Fig. 4).

Confirmation of injection sites

Immediately after the last experiments, the rats were killed with CO_2. Then 1 µl of blue ink was injected with an injection system via the guide cannulae into both OBs followed by decapitation. The OB was extracted and quickly frozen in isobutanol on dry ice and stored at -20 °C until use. Correct placement of Injection was identified on 40 µm cryostat sagittal sections stained with cresyl violet (Fig. 5c). No anatomical outliers in stereotaxic cannula implantation had to be excluded from behavioral analysis.

Video analysis: Social investigation

The analysis was done by an observer blind to the pharmacological treatment using JWatcher (downloaded from https://www.jwatcher.ucla.edu/). Thereby the duration of investigation of the stimulus rats by the experimental rats was measured. Investigation was defined as sniffing the anogenital or neck region of stimulus rats including obvious nose movements (“sniffing”). Aggressive behavior (e.g. aggressive grooming), only staying next to the stimulus rats, and rough and tumble play were where not considered investigation [4] (Fig. 5b). One animal from the control group was removed, as it showed high amounts of unspecific sexual/mounting behavior towards the stimulus animals throughout the sampling as well as the discrimination phase.

892 **Statistics and reproducibility**

893

894 Statistics were performed with SPSS (ver. 26, IBM, Armonk, NY, USA) and G*Power (ver.
895 3.1.9.2, Franz Faul, University of Kiel). All statistical analysis performed was two-sided and
896 significance was accepted at $p<0.05$. Type of statistic was determined using the Kolmogorov-
897 Smirnov test for normal distribution in SPSS. Effect sizes for parametric statistics (Cohen's *d,*
898 *dz*, *f*) were determined using SPSS and G*Power. Effect sizes for non-parametric statistics
899 were calculated from z-scores (Pearson's $r = |z|/\sqrt{n}$) [78]. Sample sizes were either based on
900 prior studies or an a priori power analysis. Power and sample sizes (for $\alpha=0.05$) were
901 determined using G*Power.
902 All Ns indicate biological replication, that is, data from different samples (different cells or
903 different animals). To better illustrate replication in acute *in-vitro* slice experiments it is also
904 clearly indicated in the results section from how many different animals the measurements
905 originate from.
906 For complete details concerning type of statistic (parametric or non-parametric), type of test,
907 test statistics (F, t, W, U, z-score), degrees of freedom, p-value, effect size, and achieved
908 power of every statistical analysis performed in the result section see table 1. Figure identifiers
909 and lower case arabic letters in the table represent affiliation to the statistical data represented
910 in the figures and the text, respectively.
911 All Ns indicate biological replication, that is, data from different samples (different cells or
912 different animals). To illustrate replication in acute *in-vitro* slice experiments it is also clearly
913 indicated in the results section from how many different animals the measurements originate
914 from.

915

916 **Data availability statement:**

917

918 All numerical data that is represented in the figures is available as source data file
919 corresponding to the figures.

Acknowledgments

The work was supported by the German research foundation (DFG LU2164/1-1 and EG 135/5-1). We thank Anne Pietryga-Krieger and Dr. Max Müller for experimental support and Dr. Mike Ludwig (University of Edinburgh) for providing the VP-eGFP rats. We also thank Prof. Inga Neumann for providing video equipment and stereotactic instruments for the behavioral pharmacology experiments and Dr. Vinicius Oliveira for critically reading the manuscript.

Author contributions

H.S. and M.L. designed research; M.L. and H.S. performed research; M.L. and H.S. analyzed data; V.E. provided advice on the design and analysis of electrophysiology and Ca^{2+} imaging experiments; H.S. wrote the first draft of the manuscript. H.S., V.E. and M.L. wrote and revised the manuscript.

Competing interest

The authors declare no competing financial interest

Table 1 **Statistical overview**

	Figure	Type of statistic	Type of test	Test statistic	P-value	Effect size	Power
a	S1a -	parametric parametric	One-way ANOVA One-way ANOVA	$F_{(2,26)}$=0.406 $F_{(2,26)}$=0.329	p=0.670 p=0.723	*f*=0.176 *f*=0.158	0.115 0.102
b	1c	parametric	One-way ANOVA and post-hoc (LSD) rat vs water rat vs urine urine vs. water	$F_{(2,26)}$=3.713 - - -	p=0.038 p=0.011 p=0.197 p=0.195	*f*=0.463 *d*=1.147 *d*=0.604 *d*=0.663	0.548
c	1e	parametric	One-way ANOVA and post-hoc (LSD) rat vs water rat vs urine urine vs. water	$F_{(2,26)}$=3.586 - - -	p=0.042 p=0.025 p=0.034 p=0.949	*f*=0.525 *d*=1.117 *d*=0.824 *d*=0.232	0.663
d	S1d	parametric	One-way ANOVA	$F_{(2,24)}$=0.633	p=0.539	*f*=0.229	0.156
e	S1e	parametric	One-way ANOVA	$F_{(2,24)}$=0.746	p=0.485	*f*=0.237	0.164
f	S1f	parametric	One-way ANOVA	$F_{(2,24)}$=1.952	p=0.164	*f*=0.403	0.404
g	2c	non-parametric	Related samples Wilcoxon test	$W_{(8)}$=0; z=-2.521	p=0.012	*r*=0.891	0.995
h	2e	non-parametric	Related samples Wilcoxon test	$W_{(9)}$=1; z=-2.547	p=0.011	*r*=0.849	0.984
i	2g	non-parametric	Related samples Wilcoxon test	$W_{(20)}$=0; z=-3.920	p<0.001	*r*=0.876	1.000
j	2h	non-parametric	Mann-Whitney-U test	z=-4.652	p<0.001	*r*=0.736	1.000
k	2i	non-parametric	Kruskal Wallis and post-hoc (Bonferroni) 5-HT vs NA ACh vs 5-HAT ACh vs NA	H=17.439, df=2 z=0.003 z=-3.433 z=-3.291	p<0.001 p=1.000 p=0.003 p=0.002	- *r*=0.001 *r*=0.649 *r*=0.611	- 0.050 0.991 0.980
l	S2a	parametric	(4) × (2) mixed model ANOVA (intensity [within subject] × treatment [within-subject])	$F_{(3, 54)}$=23.12 $F_{(1, 18)}$=0.647 $F_{(3,54)}$=0.562 (interaction)	p<0.001 p=0.432 p=0.604	*f*=1.132 *f*=0.176 *f*=0.255	1.000 0.119 0.158
m	S2b	parametric	(4) × (2) mixed model ANOVA (intensity [within subject] × treatment [within-subject]) ACh vs. ACSF with 40 pA	$F_{(3, 54)}$=52.19 $F_{(1, 18)}$=3.228 $F_{(3,54)}$=6.346 (interaction) -	p<0.001 p=0.089 p=0.010 p=0.026	*f*=1.705 *f*=0.423 *f*=0.594 *d*=1.083	1.000 0.398 0.792
n	3b	non-parametric	Related samples Wilcoxon test	$W_{(5)}$=0; z=-2.023	p=0.043	*r*=0.905	0.872
o	3d	non-parametric	Related samples Wilcoxon test	$W_{(5)}$=0; z=2.023	p=0.043	*r*=0.905	0.872
p	-	non-parametric	Mann-Whitney-U test	z=3.121	p=0.002	*r*=0.716	0.988
q	3g	parametric	(2) × (2) mixed model ANOVA (location [within subject] × treatment [within-subject])	$F_{(1,7)}$=17.8 $F_{(1,7)}$=1.98 $F_{(1,7)}$=0.014 (interaction)	p=0.004 p=0.203 p=0.910	*f*=1.596 *f*=0.531 *f*=0.045	1.000 1.000 0.081
r	S3b	parametric	(2) × (2) mixed model ANOVA (stimulation [within subject] × location [within-subject]) and post-hoc (Bonferroni) ON/soma vs. 50Hz/soma ON/soma vs. ON/tuft	$F_{(1, 7)}$=4.194 $F_{(1, 7)}$=7.446 $F_{(1,7)}$=15.01 (interaction) - -	p=0.080 p=0.029 p=0.006 p=0.014 p=0.002	*f=0.775* *f=1.030* *f=1.454* *dz=5.943* *dz=6.643*	0.424 0.650 0.911 - -
s	S3c	non-parametric	Mann-Whitney-U test	z=0.936	p=0.456	*r=0.209*	0.148
t	4b	non-parametric	Related samples Wilcoxon test	$W_{(8)}$=4; z=-0.420	p=0.327	*r=0.148*	0.065
u	4d	non-parametric	Friedman test	χ2=3.714, df=2	p=0.156	-	-
v	4f	non-parametric	Related samples Wilcoxon test	$W_{(6)}$=0; z=-2.201	p=0.028	*r=0.984*	1.000
w	4h	non-parametric	Friedman test and post-hoc (Dunn) Mecamylamine/ACh vs Mecamylamine Mecamylamine/ACh vs ACSF Mecamylamine vs ACSF	χ2=6.750, df=2 z=2.250 z=-2.250 z=0.000	p=0.034 p=0.024 p=0.024 p=1.000	- *r*=0.795 *r*=0.795 *r*=0.000	- 0.868 0.868 0.050
x	5b	parametric	One-way ANOVA	$F_{(2,13)}$=2.701	p=0.104	*f*=0.645	0.526
y	5c	parametric	One-way ANOVA and post-hoc (LSD) rat vs water	$F_{(2,13)}$=4.411 -	p=0.034 p=0.113	*f*=0.823 *d*=0.918	0.748

			rat vs urine urine vs. water	- -	p=0.011 p=0.255	*d*=1.826 *d*=0.933	
z	6d	parametric	Paired samples t-test	$t_{(12)}$=-2.411	p=0.033	*dz*=0.709	0.651
a1	6e	parametric	Paired samples t-test	$t_{(13)}$=-1.231	p=0.240	*dz*=0.202	0.208
b1	6f	parametric	Paired samples t-test	$t_{(13)}$=-2.420	p=0.031	*dz*=0.647	0.647
-	S4a	non-parametric	Kruskal-Wallis Test	H=0.341, df=2	p=0.843	-	-
-	S4b	parametric	(4) × (3) mixed model ANOVA (time bin [within subject] × treatment [within-subject])	$F_{(3,114)}$=82.09 $F_{(2,38)}$=0.599 $F_{(6,114)}$=1.144 (interaction)	p<0.001 p=0.554 p=0.224	*f=1.147* *f=0.179* *f=0.274*	1.000 0.142 0.456
-	S4c	non-parametric	Kruskal-Wallis Test	H=0.915, df=2	p=0.633	-	-
-	S4d	parametric	(4) × (3) mixed model ANOVA (time bin [within subject] × treatment [within-subject])	$F_{(3,114)}$=51.02 $F_{(2,38)}$=0.599 $F_{(6,114)}$=1.509 (interaction)	p<0.001 p=0.355 p=0.234	*f=1.161* *f=0.244* *f=0.283*	1.000 0.301 0.427

Type of statistic was determined using the Kolmogorov- Smirnov test in SPSS. Tests were performed using SPSS. Effect sizes for parametric statistics were determined using SPSS and G*Power (Cohen's *d, dz*, *f*). Effect sizes for non-parametric statistics were calculated from z-scores (Pearson's r = $|z|/\sqrt{n}$) [73]. Power (for α=0.05) was determined using G*Power.

References

1. Baldwin B, Shillito EE. The effects of ablation of the olfactory bulbs on parturition and maternal behaviour in Soay sheep. *Animal Behaviour* **22**, 220-223 (1974).

2. Williams JR, Slotnick BM, Kirkpatrick BW, Carter CS. Olfactory-Bulb Removal Affects Partner Preference Development and Estrus Induction in Female Prairie Voles. *Physiology & Behavior* **52**, 635-639 (1992).

3. Matsuo T*, et al.* Genetic dissection of pheromone processing reveals main olfactory system-mediated social behaviors in mice. *P Natl Acad Sci USA* **112**, E311-E320 (2015).

4. Engelmann M, Hadicke J, Noack J. Testing declarative memory in laboratory rats and mice using the nonconditioned social discrimination procedure. *Nature Protocols* **6**, 1152-1162 (2011).

5. Lukas M, Neumann ID. Oxytocin and vasopressin in rodent behaviors related to social dysfunctions in autism spectrum disorders. *Behav Brain Res* **251**, 85-94 (2013).

6. Dluzen DE, Muraoka S, Engelmann M, Landgraf R. The effects of infusion of arginine vasopressin, oxytocin, or their antagonists into the olfactory bulb upon social recognition responses in male rats. *Peptides* **19**, 999-1005 (1998).

7. Tobin VA*, et al.* An intrinsic vasopressin system in the olfactory bulb is involved in social recognition. *Nature* **464**, 413-U110 (2010).

8. Lukas M, Suyama H, Egger V. Vasopressin Cells in the Rodent Olfactory Bulb Resemble Non-Bursting Superficial Tufted Cells and Are Primarily Inhibited upon Olfactory Nerve Stimulation. *eneuro* **6**, ENEURO.0431-0418.2019 (2019).

9. Halász N. *The Vertebrate Olfactory System: Chemical neuroanatomy, function and development*. Akadémiai Kiadó (1990).

10. Bobrov E, Wolfe J, Rao RP, Brecht M. The Representation of Social Facial Touch in Rat Barrel Cortex. *Current Biology* **24**, 109-115 (2014).

11. Shipley MT, Halloran FJ, Delatorre J. Surprisingly Rich Projection from Locus Coeruleus to the Olfactory-Bulb in the Rat. *Brain Research* **329**, 294-299 (1985).

12. McLean JH, Shipley MT. Serotonergic afferents to the rat olfactory bulb: I. Origins and laminar specificity of serotonergic inputs in the adult rat. *Journal of Neuroscience* **7**, 3016-3028 (1987).

13. Ojima H, Yamasaki T, Kojima H, Akashi A. Cholinergic Innervation of the Main and the Accessory Olfactory Bulbs of the Rat as Revealed by a Monoclonal-Antibody against Choline-Acetyltransferase. *Anatomy and Embryology* **178**, 481-488 (1988).

14. Popova NK, Amstislavskaya TG. 5-HT2A and 5-HT2C serotonin receptors differentially modulate mouse sexual arousal and the hypothalamo-pituitary-testicular response to the presence of a female. *Neuroendocrinology* **76**, 28-34 (2002).

15. Purvis EM, Klein AK, Ettenberg A. Lateral habenular norepinephrine contributes to states of arousal and anxiety in male rats. *Behavioural Brain Research* **347**, 108-115 (2018).

16. Acquas E, Wilson C, Fibiger HC. Conditioned and unconditioned stimuli increase frontal cortical and hippocampal acetylcholine release: Effects of novelty, habituation, and fear. *Journal of Neuroscience* **16**, 3089-3096 (1996).

17. Prado VF*, et al.* Mice deficient for the vesicular acetylcholine transporter are myasthenic and have deficits in object and social recognition. *Neuron* **51**, 601-612 (2006).

18. Dluzen DE, Muraoka S, Landgraf R. Olfactory bulb norepinephrine depletion abolishes vasopressin and oxytocin preservation of social recognition responses in rats. *Neuroscience Letters* **254**, 161-164 (1998).

19. Cavalcante LES*, et al.* Modulation of the storage of social recognition memory by neurotransmitter systems in the insular cortex. *Behavioural Brain Research* **334**, 129-134 (2017).

20. Ueta Y*, et al.* Transgenic expression of enhanced green fluorescent protein enables direct visualization for physiological studies of vasopressin neurons and isolated nerve terminals of the rat. *Endocrinology* **146**, 406-413 (2005).

21. Bluthe RM, Dantzer R. Role of the Vomeronasal System in Vasopressinergic Modulation of Social Recognition in Rats. *Brain Research* **604**, 205-210 (1993).

22. Le Jeune H, Aubert I, Jourdan F, Quirion R. Comparative laminar distribution of various autoradiographic cholinergic markers in adult rat main olfactory bulb. *Journal of chemical neuroanatomy* **9**, 99-112 (1995).

23. Yuan Q, Harley CW, McLean JH. Mitral cell β1 and 5-HT2A receptor colocalization and cAMP coregulation: A new model of norepinephrine-induced learning in the olfactory bulb. *Learning & memory* **10**, 5-15 (2003).

24. Vargas-Barroso V, Ordaz-Sánchez B, Peña-Ortega F, Larriva-Sahd JA. Electrophysiological Evidence for a Direct Link between the Main and Accessory Olfactory Bulbs in the Adult Rat. *Frontiers in Neuroscience* **9**, 518 (2016).

25. Noack J, Richter K, Laube G, Haghgoo HA, Veh RW, Engelmann M. Different importance of the volatile and non-volatile fractions of an olfactory signature for individual social recognition in rats versus mice and short-term versus long-term memory. *Neurobiology of Learning and Memory* **94**, 568-575 (2010).

26. Liu SL, Shao ZY, Puche A, Wachowiak M, Rothermel M, Shipley MT. Muscarinic Receptors Modulate Dendrodendritic Inhibitory Synapses to Sculpt Glomerular Output. *Journal of Neuroscience* **35**, 5680-5692 (2015).

27. Shipley MT, Ennis M. Functional organization of olfactory system. *Journal of Neurobiology* **30**, 123-176 (1996).

28. Bains JS, Ferguson AV. Activation of N-methyl-d-aspartate receptors evokes calcium spikes in the dendrites of rat hypothalamic paraventricular nucleus neurons. *Neuroscience* **90**, 885-891 (1999).

29. Senut M, Menetrey D, Lamour Y. Cholinergic and peptidergic projections from the medial septum and the nucleus of the diagonal band of Broca to dorsal hippocampus, cingulate cortex and olfactory bulb: a combined wheatgerm agglutinin-apohorseradish peroxidase-gold immunohistochemical study. *Neuroscience* **30**, 385-403 (1989).

30. Schwarz I*, et al.* The diagonal band of broca continually regulates olfactory-mediated behaviors by modulating odor-evoked responses within the olfactory bulb. *bioRxiv*, 2020.2011.2007.372649 (2020).

31. Linster C, Hasselmo ME. Neural activity in the horizontal limb of the diagonal band of Broca can be modulated by electrical stimulation of the olfactory bulb and cortex in rats. *Neuroscience Letters* **282**, 157-160 (2000).

32. Zhu XO, Brown MW, Mccabe BJ, Aggleton JP. Effects of the Novelty or Familiarity of Visual-Stimuli on the Expression of the Immediate-Early Gene C-Fos in Rat-Brain. *Neuroscience* **69**, 821-829 (1995).

33. McKenna JT*, et al.* c-Fos protein expression is increased in cholinergic neurons of the rodent basal forebrain during spontaneous and induced wakefulness. *Brain Research Bulletin* **80**, 382-388 (2009).

34. Imperato A, Puglisiallegra S, Scrocco MG, Casolini P, Bacchi S, Angelucci L. Cortical and Limbic Dopamine and Acetylcholine-Release as Neurochemical Correlates of Emotional Arousal in Both Aversive and Non-Aversive Environmental-Changes. *Neurochemistry International* **20**, S265-S270 (1992).

35. Passetti F, Dalley JW, O'connell MT, Everitt BJ, Robbins TW. Increased acetylcholine release in the rat medial prefrontal cortex during performance of a visual attentional task. *European Journal of Neuroscience* **12**, 3051-3058 (2000).

36. Butt AE, Testylier G, Dykes RW. Acetylcholine release in rat frontal and somatosensory cortex is enhanced during tactile discrimination learning. *Psychobiology* **25**, 18-33 (1997).

37. Bohm E, Brunert D, Rothermel M. Input dependent modulation of olfactory bulb activity by HDB GABAergic projections. *Scientific Reports* **10**, 1-15 (2020).

38. Rothermel M, Carey RM, Puche A, Shipley MT, Wachowiak M. Cholinergic Inputs from Basal Forebrain Add an Excitatory Bias to Odor Coding in the Olfactory Bulb. *Journal of Neuroscience* **34**, 4654-4664 (2014).

39. Anagnostaras SG*, et al.* Selective cognitive dysfunction in acetylcholine M-1 muscarinic receptor mutant mice. *Nature Neuroscience* **6**, 51-58 (2003).

40. Mirich JM, Illig KR, Brunjes PC. Experience‐dependent activation of extracellular signal‐related kinase (ERK) in the olfactory bulb. *Journal of comparative Neurology* **479**, 234-241 (2004).

41. Wacker DW, Engelmann M, Tobin VA, Meddle SL, Ludwig M. Vasopressin and social odor processing in the olfactory bulb and anterior olfactory nucleus. *Ann Ny Acad Sci* **1220**, 106-116 (2011).

42. Haga S*, et al.* The male mouse pheromone ESP1 enhances female sexual receptive behaviour through a specific vomeronasal receptor. *Nature* **466**, 118-U136 (2010).

43. Hattori T*, et al.* Self-Exposure to the Male Pheromone ESP1 Enhances Male Aggressiveness in Mice. *Current Biology* **26**, 1229-1234 (2016).

44. Kaba H, Rosser A, Keverne B. Neural Basis of Olfactory Memory in the Context of Pregnancy Block. *Neuroscience* **32**, 657-662 (1989).

45. Baum MJ, Kelliher KR. Complementary Roles of the Main and Accessory Olfactory Systems in Mammalian Mate Recognition. *Annual Review of Physiology* **71**, 141-160 (2009).

46. Gregg CM. The Compartmentalized Hypothalamo-Neurohypophysial System: Evidence for a NeurohypophysialAction of Acetylcholine on Vasopressin Release. *Neuroendocrinology* **40**, 423-429 (1985).

47. Li DP, Pan YZ, Pan HL. Acetylcholine attenuates synaptic GABA release to supraoptic neurons through presynaptic nicotinic receptors. *Brain Research* **920**, 151-158 (2001).

48. Ravel N, Akaoka H, Gervais R, Chouvet G. The Effect of Acetylcholine on Rat Olfactory-Bulb Unit-Activity. *Brain Research Bulletin* **24**, 151-155 (1990).

49. Matsutani S, Yamamoto N. Centrifugal innervation of the mammalian olfactory bulb. *Anatomical Science International* **83**, 218-227 (2008).

50. Bendahmane M, Ogg MC, Ennis M, Fletcher ML. Increased olfactory bulb acetylcholine bi-directionally modulates glomerular odor sensitivity. *Scientific reports* **6**, 25808 (2016).

51. Quick MW, Lester RAJ. Desensitization of neuronal nicotinic receptors. *Journal of Neurobiology* **53**, 457-478 (2002).

52. D'Souza RD, Vijayaraghavan S. Nicotinic receptor-mediated filtering of mitral cell responses to olfactory nerve inputs involves the α3β4 subtype. *Journal of Neuroscience* **32**, 3261-3266 (2012).

53. Rao RP, Mielke F, Bobrov E, Brecht M. Vocalization–whisking coordination and multisensory integration of social signals in rat auditory cortex. *Elife* **3**, e03185 (2014).

54. Chaves-Coira I, Rodrigo-Angulo ML, Nunez A. Bilateral Pathways from the Basal Forebrain to Sensory Cortices May Contribute to Synchronous Sensory Processing. *Frontiers in Neuroanatomy* **12**, 5 (2018).

55. Kirkwood A, Rozas C, Kirkwood J, Perez F, Bear MF. Modulation of long-term synaptic depression in visual cortex by acetylcholine and norepinephrine. *Journal of Neuroscience* **19**, 1599-1609 (1999).

56. Metherate R, Ashe JH. Synaptic-Interactions Involving Acetylcholine, Glutamate, and Gaba in Rat Auditory-Cortex. *Experimental Brain Research* **107**, 59-72 (1995).

57. Butt AE*, et al.* Association learning-dependent increases in acetylcholine release in the rat auditory cortex during auditory classical conditioning. *Neurobiology of Learning and Memory* **92**, 400-409 (2009).

58. Rogers-Carter MM, Christianson JP. An insular view of the social decision-making network. *Neurosci Biobehav R* **103**, 119-132 (2019).

59. Baez S, García AM, Ibanez A. The Social Context Network Model in Psychiatric and Neurological Diseases. In: *Social Behavior from Rodents to Humans: Neural Foundations and Clinical Implications* (ed^(eds Wöhr M, Krach S). Springer International Publishing (2017).

60. Giovannini MG, Rakovska A, Benton RS, Pazzagli M, Bianchi L, Pepeu G. Effects of novelty and habituation on acetylcholine, GABA, and glutamate release from the frontal cortex and hippocampus of freely moving rats. *Neuroscience* **106**, 43-53 (2001).

61. Wilson DA, Fletcher ML, Sullivan RM. Acetylcholine and olfactory perceptual learning. *Learning & Memory* **11**, 28-34 (2004).

62. Ravel N, Elaagouby A, Gervais R. Scopolamine Injection into the Olfactory-Bulb Impairs Short-Term Olfactory Memory in Rats. *Behavioral Neuroscience* **108**, 317-324 (1994).

63. Ross JM, Bendahmane M, Fletcher ML. Olfactory Bulb Muscarinic Acetylcholine Type 1 Receptors Are Required for Acquisition of Olfactory Fear Learning. *Frontiers in Behavioral Neuroscience* **13**, (2019).

64. Mandairon N, Ferretti CJ, Stack CM, Rubin DB, Cleland TA, Linster C. Cholinergic modulation in the olfactory bulb influences spontaneous olfactory discrimination in adult rats. *European Journal of Neuroscience* **24**, 3234-3244 (2006).

65. Martinon D*, et al.* Oxytocin receptors in the dorsolateral bed nucleus of the stria terminalis (BNST) bias fear learning toward temporally predictable cued fear. *Translational Psychiatry* **9**, 140 (2019).

66. de la Zerda SH*, et al.* Social recognition in rats and mice requires integration of olfactory, somatosensory and auditory cues. *bioRxiv*, (2020).

67. Singer AG, Beauchamp GK, Yamazaki K. Volatile signals of the major histocompatibility complex in male mouse urine. *P Natl Acad Sci USA* **94**, 2210-2214 (1997).

68. Yokoi M, Mori K, Nakanishi S. Refinement of Odor Molecule Tuning by Dendrodendritic Synaptic Inhibition in the Olfactory-Bulb. *P Natl Acad Sci USA* **92**, 3371-3375 (1995).

69. Cleland TA, Sethupathy P. Non-topographical contrast enhancement in the olfactory bulb. *Bmc Neuroscience* **7**, 1-18 (2006).

70. Paxinos G, Watson C. The rat brain in stereotaxic coordinates: compact sixth edition. (ed^(eds). New York: Academic Press (2009).

71. Egger V, Svoboda K, Mainen ZF. Mechanisms of lateral inhibition in the olfactory bulb: efficiency and modulation of spike-evoked calcium influx into granule cells. *Journal of Neuroscience* **23**, 7551-7558 (2003).

72. Pignatelli A, Belluzzi O. Cholinergic modulation of dopaminergic neurons in the mouse olfactory bulb. *Chemical Senses* **33**, 331-338 (2008).

73. Liu S, Aungst JL, Puche AC, Shipley MT. Serotonin modulates the population activity profile of olfactory bulb external tufted cells. *Journal of neurophysiology* **107**, 473-483 (2011).

74. Zimnik NC, Treadway T, Smith RS, Araneda RC. α1A‐Adrenergic regulation of inhibition in the olfactory bulb. *The Journal of physiology* **591**, 1631-1643 (2013).

75. Castillo PE, Carleton A, Vincent J-D, Lledo P-M. Multiple and opposing roles of cholinergic transmission in the main olfactory bulb. *Journal of Neuroscience* **19**, 9180-9191 (1999).

76. Sun YG*, et al.* Biphasic cholinergic synaptic transmission controls action potential activity in thalamic reticular nucleus neurons. *J Neurosci* **33**, 2048-2059 (2013).

77. Saboory E, Gholami M, Zare S, Roshan‐Milani S. The long‐term effects of neonatal morphine administration on the pentylenetetrazol seizure model in rats: The role of hippocampal cholinergic receptors in adulthood. *Developmental psychobiology* **56**, 498-509 (2014).

78. Rosenthal R, Cooper H, Hedges L. Parametric measures of effect size. *The handbook of research synthesis* **621**, 231-244 (1994).